EUROPEAN ORGANIZATION FOR NUCLEAR RESEARCH

Status report of the HARP experiment October 2008

CERN-SPSC-2008-030 / SPSC-SR-038
03/11/2008

The HARP Collaboration

29 October 2008

HARP collaboration

M.G. Catanesi, E. Radicioni
Università degli Studi e Sezione INFN, Bari, Italy
R. Edgecock, M. Ellis[1], F.J.P. Soler[2]
Rutherford Appleton Laboratory, Chilton, Didcot, UK
C. Gößling
Institut für Physik, Universität Dortmund, Germany
S. Bunyatov, A. Krasnoperov, B. Popov[3], V. Serdiouk, V. Tereshchenko
Joint Institute for Nuclear Research, JINR Dubna, Russia
E. Di Capua, G. Vidal–Sitjes[4]
Università degli Studi e Sezione INFN, Ferrara, Italy
A. Artamonov[5], S. Giani, S. Gilardoni, P. Gorbunov[5], A. Grant, A. Grossheim[7], V. Ivanchenko[8],
A. Kayis-Topaksu[9], J. Panman, I. Papadopoulos, E. Tcherniaev, I. Tsukerman[5], R. Veenhof,
C. Wiebusch[10], P. Zucchelli[6,11]
CERN, Geneva, Switzerland
A. Blondel, S. Borghi[12], M.C. Morone[13], G. Prior[14], R. Schroeter
Section de Physique, Université de Genève, Switzerland
C. Meurer
Institut für Physik, Forschungszentrum Karlsruhe, Germany
U. Gastaldi
Laboratori Nazionali di Legnaro dell' INFN, Legnaro, Italy
G. B. Mills[15]
Los Alamos National Laboratory, Los Alamos, USA
J.S. Graulich[16], G. Grégoire
Institut de Physique Nucléaire, UCL, Louvain-la-Neuve, Belgium
M. Bonesini, F. Ferri
Università degli Studi e Sezione INFN, Milano, Italy
M. Kirsanov
Institute for Nuclear Research, Moscow, Russia
A. Bagulya, V. Grichine, N. Polukhina
P. N. Lebedev Institute of Physics (FIAN), Russian Academy of Sciences, Moscow, Russia
V. Palladino
Università "Federico II" e Sezione INFN, Napoli, Italy
L. Coney[15], D. Schmitz[15]
Columbia University, New York, USA
G. Barr, A. De Santo[17]
Nuclear and Astrophysics Laboratory, University of Oxford, UK
F. Bobisut, D. Gibin, A. Guglielmi, M. Mezzetto
Università degli Studi e Sezione INFN, Padova, Italy
J. Dumarchez
LPNHE, Universités de Paris VI et VII, Paris, France
U. Dore
Università "La Sapienza" e Sezione INFN Roma I, Roma, Italy
D. Orestano, F. Pastore, A. Tonazzo, L. Tortora
Università degli Studi e Sezione INFN Roma III, Roma, Italy
C. Booth, L. Howlett
Dept. of Physics, University of Sheffield, UK
M. Bogomilov, M. Chizhov, D. Kolev, R. Tsenov
Faculty of Physics, St. Kliment Ohridski University, Sofia, Bulgaria
S. Piperov, P. Temnikov
Institute for Nuclear Research and Nuclear Energy, Academy of Sciences, Sofia, Bulgaria
M. Apollonio, P. Chimenti, G. Giannini
Università degli Studi e Sezione INFN, Trieste, Italy
J. Burguet–Castell, A. Cervera–Villanueva, J.J. Gómez–Cadenas, J. Martín–Albo, P. Novella, M. Sorel
Instituto de Física Corpuscular, IFIC, CSIC and Universidad de Valencia, Spain

[1]Now at Brunel University, Uxbridge, England.
[2]Now at University of Glasgow, UK.
[3]Also supported by LPNHE, Paris, France.
[4]Now at Imperial College, University of London, UK.
[5]ITEP, Moscow, Russian Federation.
[6]Now at SpinX Technologies, Geneva, Switzerland.
[7]Now at TRIUMF, Vancouver, Canada.
[8]On leave of absence from Ecoanalitica, Moscow State University, Moscow, Russia.
[9]Now at Çukurova University, Adana, Turkey.
[10]Now at III Phys. Inst. B, RWTH Aachen, Aachen, Germany.
[11]On leave of absence from INFN, Sezione di Ferrara, Italy.
[12]Now at CERN, Geneva, Switzerland.
[13]Now at Univerity of Rome Tor Vergata, Italy.
[14]Now at Lawrence Berkeley National Laboratory, Berkeley, California, USA.
[15]MiniBooNE Collaboration.
[16]Now at Section de Physique, Université de Genève, Switzerland, Switzerland.
[17]Now at Royal Holloway, University of London, UK.

Abstract

The current status of the HARP experiment is shortly described, emphasizing the developments since the previous status report, which was presented in September 2007 [1].

The final results of the measurement of positive pion production in the p–Al interactions at 12.9 GeV/c with the forward spectrometer relevant for the K2K experiment [2] and the measurement of charged pion production for the MiniBooNE experiment [3] (8.9 GeV/c p–Be interactions) have been published [4, 5]. They will be only briefly mentioned here. A new application of HARP data arises after the approval of the SciBooNE experiment [6], which has taken data in the same neutrino (antineutrino) beam as used by MiniBooNE.

The analysis for the determination of the charged pion production cross-sections in p–C and $\pi^{\pm}$–C interactions relevant for the precise calculation of atmospheric neutrino flux and simulation of extended air showers was published [7]. Recently results using N_2 and O_2 cryogenic targets were also obtained and published [8].

In addition final results on the measurements of the double-differential cross-section, $\mathrm{d}^2\sigma^{\pi}/\mathrm{d}p\mathrm{d}\Omega$, for $\pi^{\pm}$ forward production by incident charged pions of 3 GeV/c, 5 GeV/c, 8 GeV/c and 12 GeV/c momentum impinging on a thin beryllium, carbon, aluminum, copper, tin, tantalum or lead target have been obtained [9]. The corresponding paper has recently been accepted for publication in Nucl. Phys. A.

In our previous SPSC report we reported in details about the full set of calibration methods for the TPC and RPC and the corresponding reconstruction and simulation software. The combined effect of the distortions on the kinematic quantities has been studied in detail. As a pragmatic approach only early part of the beam spill (more than 30% of the data) for which the effects of dynamic distortions are still small and systematic errors can be controlled with physical benchmarks was used first [10, 11, 12, 13]. The measurements of charged pion yields in p–Ta interactions based on those methods as well as similar results obtained using different targets (Be, C, Al, Cu, Sn, Pb) and proton beam momenta of 3, 5, 8 and 12 GeV/c, are now published [10, 14, 15].

Further, methods to correct the dynamic distortions have been developed [11, 16] and are currently applied in the ongoing analyses. A systematic study of production cross-sections with a wide range of nuclear targets, using protons, π^+ and π^- beams with momentum of 3, 5, 8 and 12 GeV/c and making use of the full data sample available in the spill was performed. The results for the incoming proton beam have been already published [17]. The analyses using π^+ and π^- beams are also completed and will be submitted for publication soon.

The last section of this report is devoted to the comparisons of our large angle results with previously published data and some recent results of an alternative analysis performed by the so-called CDP group.

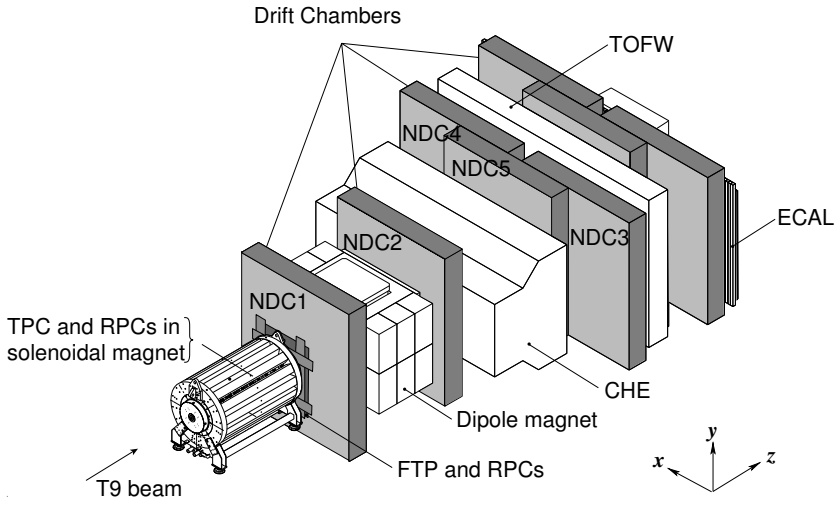

Figure 1: Schematic layout of the HARP spectrometer

1 Introduction

The objective of the HARP experiment is a systematic study of hadron production for beam momenta from 1.5 GeV/c to 15 GeV/c for a large range of target nuclei [18]. The main motivations are the measurement of pion yields for a quantitative design of the proton driver of a future neutrino factory, a substantial improvement of the calculation of the atmospheric neutrino flux and the measurement of particle yields as input for the flux calculation of accelerator neutrino experiments, such as K2K and MiniBooNE.

The HARP experiment [18, 19, 20] (Fig. 1) makes use of a large-acceptance spectrometer consisting of a forward and large-angle detection systems. The forward spectrometer covers polar angles up to 250 mrad which is well matched to the angular range of interest for the measurement of hadron production to calculate the properties of conventional neutrino beams. In particular, it matches the acceptance of the K2K and MiniBooNE beam lines. It uses a dipole magnet and large planar drift chambers for particle tracking. In addition, the particle identification is performed with a combination of time-of-flight, Cherenkov, and calorimeter information. In the large-angle region a TPC positioned in a solenoidal magnet is used for tracking. Particle identification is performed with the $\mathrm{d}E/\mathrm{d}x$ in the TPC and the time-of-flight measurements with RPCs. The large-angle spectrometer has an acceptance which is optimized for the measurement of pions relevant to the production of muons in future neutrino factories. It has a large acceptance in the momentum and angular range for the pions. It covers 90% of the pions accepted in the focusing system of a typical design. In addition, beam instrumentation (including three timing detectors and two threshold Cherenkov detectors) provides identification of the incoming particle and the determination of the interaction time at the target. The impact point on the target is measured by a set of beam multi-wire proportional chambers (MWPCs). The results reported here are based on data taken in 2002 in the T9 beam of the CERN PS.

This report summarizes the progress of HARP since the previous status report of September 2007 [1].

The final result of the measurement of positive pion production for the K2K experiment with the forward spectrometer has been published [4] and used for the analysis of the K2K data [21, 2]. These results had been shown in the previous report and will be only briefly mentioned here.

The analysis of the data in view of the measurement of charged pion production for the MiniBooNE experiment (8.9 GeV/c p–Be interactions) has also been published [5] and the measured production spectra are being used by the MiniBooNE collaboration and are included in their recent publication [3]. A new application of HARP data arises after the approval of the SciBooNE experiment [6], which has taken data in the same neutrino beam used by MiniBooNE in order to perform a precision measurement of neutrino cross sections in the neutrino energy region around 1 GeV. Both experiments used also the antineutrino mode and will profit a lot from the knowledge of the π^- secondary production. This result was also achieved by HARP. A paper on the full characterization of the neutrino (antineutrino) beam at FERMILAB (actually in preparation) will include these HARP results [22].
The analysis for the determination of the charged pion production cross-sections in p–C and $\pi^{\pm}$–C interactions relevant for the precise calculation of atmospheric neutrino flux and simulation of extended air showers was published [7]. Recently results using N_2 and O_2 cryogenic targets were also obtained and published [8].
These results will be summarized in this document.
In the previous report we reported in details about the full set of calibration methods for the TPC and RPC and the corresponding reconstruction and simulation software. For the first analyses a different pragmatic approach was chosen and only the early part of the beam spill (more than 30% of the data) where the effects of dynamic distortions are still small was used. The combined effect of the distortions on the kinematic quantities used in the analysis has been studied in detail, and only that part of the data for which the systematic errors can be controlled with physical benchmarks were used.
The measurements based on those methods of pions yields in p–Ta interactions and similar results obtained using several different targets (Be, C, Al, Cu, Sn, Pb) and proton beams of 3, 5, 8 and 12 GeV/c, are now published [10, 14, 15]. They were described in detail in the previous report. We will recall them here only briefly.

Further, methods to correct the dynamic distortions have been developed [11, 16] and are currently applied in the ongoing analyses. A systematic study of production cross-sections with a large range of different targets, using protons, π^+ and π^- beams with momentum of 3, 5, 8 and 12 GeV/c and making use of the full data sample available in the spill was performed and the corresponding results using proton's beam have been published [17]. The same paper includes an exhaustived comparison between the data and the major publicly available hadronic generators [23, 24]. The analyses using π^+ and π^- beams were also completed and will be submitted for publication soon.
The last section of this report is devoted to the comparison with previously published data and some recent results of an alternative analysis performed by the so-called CDP group.

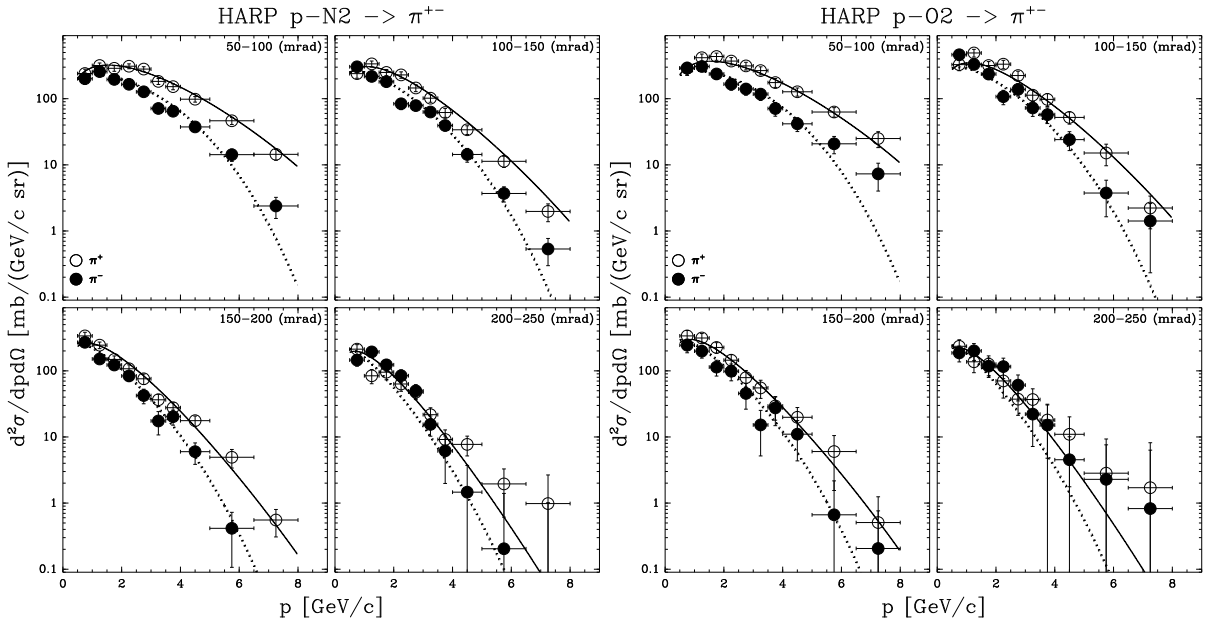

Figure 2: Measurement of the double-differential production cross-section of positive (open circles) and negative (filled circles) pions from 12 GeV/c protons on N_2 (left) and O_2 (right) as a function of pion momentum, p, in bins of pion angle, θ, in the laboratory frame. The curves show the Sanford-Wang parametrization with the parameters given in Ref. [7] (solid line for π^+ and dashed line for π^-), computed for the central value of each angular bin. In the top right corner of each plot the covered angular range is shown in mrad.

2 Results obtained with the HARP forward spectrometer

2.1 The Forward analysis.

During 2008 the collaboration has concentrated on the analysis of data with thin Carbon and cryogenic (O_2, N_2) targets relevant for atmospheric neutrino flux and extended air showers (EAS) simulation. We have also finalized the analysis on the production of pions on full set of nuclear targets with incident $\pi^{\pm}$. These results have recently been accepted for publication in Nucl. Phys. A [9]. In addition further analysis and papers are on the way, e.g. a forthcoming paper will include the results on pion production on nuclear targets with incident protons.
For a detailed description of the experimental techniques used for data analysis in the HARP forward spectrometer see Ref. [4, 5, 20].

2.2 Analysis of data with carbon or cryogenic targets

Carbon is an isoscalar nucleus as nitrogen and oxygen, so the extrapolation to air is the most straightforward. Unfortunately, the existing data for a carbon target at low energies are very scarce and cover only a very small part of the secondary particle phase space of interest to the calculation of the atmospheric neutrino fluxes and to EAS modeling.

It is more difficult for experiments to study p–O_2 and p–N_2 reactions because cryogenic targets are more complicated to handle.

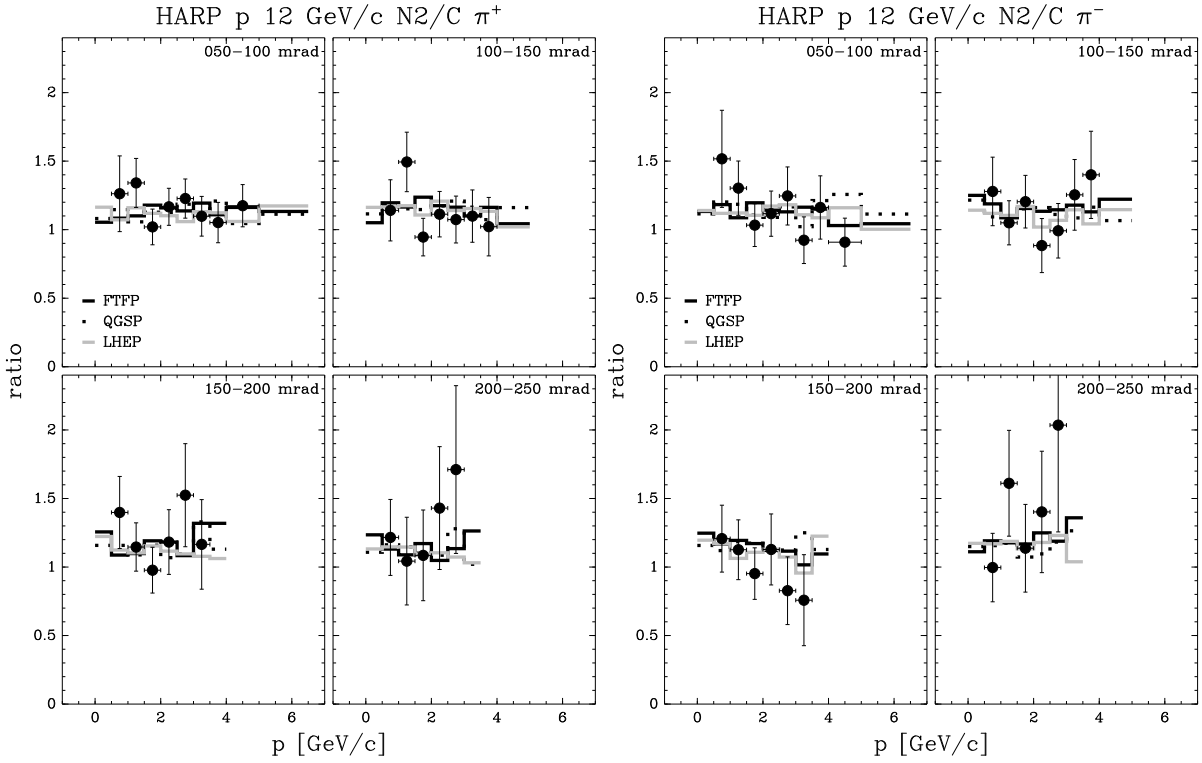

Figure 3: Ratio of p–N_2 to p–C production for π^+(left panel) and π^-(right panel) at 12 GeV/c compared with GEANT4 predictions using different models. In the top right corner of each plot the covered angular range is shown in mrad. Only statistical errors are used since most of systematics cancel.

Measurements of the double-differential cross-section, $\mathrm{d}^2\sigma^\pi/\mathrm{d}p\mathrm{d}\Omega$, for positive and negative pion production (in the kinematic range of momentum 0.5 GeV/$c \leq p_\pi <$ 8 GeV/c and angle 50 mrad $\leq \theta_\pi <$ 250 mrad in the laboratory frame) by protons of 12 GeV/c momentum impinging on thin cryogenic N_2 and O_2 targets and solid C target have been recently published [7, 8].

These results will significantly contribute to the precise calculations of atmospheric neutrino fluxes and to the improvement of our understanding of extensive air shower simulations and hadronic interactions at low energies.

One year ago we reported about the results obtained using the thin Carbon target.
Here we show the results published in [8] where for the first time measurements with cryogenic targets with good precision were obtained in this kinematic region.

In Figure 2, the measured π^+ and π^- spectra in p–N_2 and p–O_2 interactions at 12 GeV/c are compared to those measured in p–C interactions. The comparison is performed by using an empirical parametrization, developed by Sanford and Wang [25] to describe the production cross-sections of mesons in proton-nucleus interactions. The parameters fitted to our p–C data at 12 GeV/c in [7] have been used and only a constant overall rescaling factor accounting for the target atomic mass has been applied. One can observe that the shape and normalization obtained using the carbon data predict quite well the nitrogen and oxygen data. This point will be made more clear when the N_2/C and O_2/C ratios are taken. The shapes of the momentum spectra are similar for secondary π^+ and π^-, as well as for different data sets, where only a different normalization factor can be noticed because of the different nuclear masses of the

target nuclei. The conclusions drawn in [7] appear to be confirmed for the data sets presented here: the parametrization provides an approximate description of the main features, but is not able to describe the data well in some regions of kinematic space, particularly at high momenta and at large angles.
As example the pion production ratios N_2/C is presented in Figs. 3 compared to GEANT4 Monte Carlo predictions. As noted before, the difference between the target materials is justified by an overall normalization factor taking into account the different nuclear masses of the target materials. The various models predict the ratio of cross-sections accurately, with very little spread between them. Vice-versa, this is not true if one compares the absolute predictions of these models with the measured cross-sections as shown in Ref. [7].

2.3 Analysis on nuclear targets with incident pions

Measurements with incident charged pions are of great interest for the calculation of cosmic-ray muon and neutrino fluxes using extended air shower simulations. In addition these data are important to simulate re-interactions in particle detectors and neutrino beam production targets. At present these calculations rely on models with large uncertainties given the lack of experimental data in the momentum region below 15 GeV/c.

HARP is the first experiment to provide a high statistics data set, taken with many different targets, full particle identification and large detector acceptance.

The paper [9] presents our final measurements of the double-differential cross-section, $\mathrm{d}^2\sigma^\pi/\mathrm{d}p\mathrm{d}\Omega$, for $\pi^\pm$ forward production by incident charged pions of 3 GeV/c, 5 GeV/c, 8 GeV/c and 12 GeV/c momentum impinging on a thin beryllium, carbon, aluminum, copper, tin, tantalum or lead target. Some plots extracted from this paper are available in the Appendix.

The measured double-differential cross-sections for the production of π^+ and π^- in the laboratory system as a function of the momentum and the polar angle for each incident beam momentum are shown in Figure 17 for a typical target (Cu). Similar results have been obtained for thin Be, Al, C, Sn, Pb and Ta targets. The error bars shown are the square-roots of the diagonal elements in the covariance matrix, where statistical and systematic uncertainties are combined in quadrature. The correlation of the statistical errors (introduced by the unfolding procedure) are typically smaller than 20% for adjacent momentum bins and even smaller for adjacent angular bins. The correlations of the systematic errors are larger, typically 80% for adjacent bins. The overall scale error ($< 2\%$) is not shown.

The dependence of the averaged pion yields on the atomic number A is shown in Figs. 18 and 19. The π^- yields, averaged over two angular regions (0.05 rad $\leq \theta <$ 0.15 rad and 0.15 rad $\leq \theta <$ 0.25 rad) and four momentum regions (0.5 GeV/$c \leq p <$ 1.5 GeV/c, 1.5 GeV/$c \leq p <$ 2.5 GeV/c, 2.5 GeV/$c \leq p <$ 3.5 GeV/c and 3.5 GeV/$c \leq p <$ 4.5 GeV/c), are shown in the left panel and the π^+ data averaged over the same regions in the right panel, for four different beam momenta. One observes a smooth behavior of the averaged yields. The A-dependence is slightly different for π^- and π^+ production, the latter saturating earlier towards higher A, especially at lower beam momenta.

HARP data were compared with publicly available Monte Carlo generators: GEANT4 [23] and MARS [24], not previously tuned to our data-sets by using different models. The comparison was done for a limited set of plots and only for the Be and Ta targets, as examples of a light

and a heavy target. Figure 20 just shows one example of these comparisons.

Data have been compared to the available models, first renormalizing MC predictions to data and then computing the χ^2 between models and data themselves. Over the full energy range, covered by the HARP experiment, the best comparison is obtained with the MARS Monte Carlo that is on average 10% below the data, with a maximum shift of 30%. Unfortunately, all models have very bad χ^2 compared with the data, showing severe inconsistencies in the shape distribution. This is worse than the situation with incident protons and may be explained by the fact that in the latter case some experimental data were available previously to tune the Monte Carlo simulations. This was not the situation with incident pions in this energy range (below 15 GeV/c) where no earlier data can be found.

At higher energies the FTP model (from GEANT4) and the MARS model describe the data better, while at the lowest energies the Bertini and binary cascade models (from GEANT4) seem more appropriate. Parametrized models, such as LHEP from GEANT4, show relevant discrepancies.

We stress that the HARP data reported in [9] are the first precision measurements with incoming charged pion beams in the kinematic region below 15 GeV/c and may have a major impact on the tuning of Monte Carlo generators at low energies.

3 Results obtained with the HARP Large Angle spectrometer

Pion production data at low momenta ($\simeq$ 200 MeV/c) are extremely scarce and HARP is the first experiment to provide a large data set, taken with many different targets, full particle identification and large acceptance detector. In addition, the acceptance of the large-angle spectrometer of the HARP experiment matches well the required phase space region of pions relevant to the production of μ's in a neutrino factory (NF). It covers the large majority of the pions accepted in the focusing system of a typical design. For the optimization of the NF target, data were taken with high-Z nuclear targets such as tantalum and lead.

3.1 Full spill

A first set of results on the production of pions at large angles have been published by the HARP Collaboration in references [10, 14, 15], based on the analysis of the data in the beginning of each accelerator spill. The reduction of the data set was necessary to avoid problems in the TPC detector responsible for dynamic distortions to the image of the particle trajectories as the ion charge was building up during each spill. Software methods that allow the use of the full statistics, correcting for such distortions, have been developed in [11] and are fully applied in our analysis. The obtained results are compatible within the statistical errors and differential systematic uncertainties with those previously published. The increase of statistics was particularly useful in the 3 GeV/c data sets.

The analysis of the production of pions at large angles with respect to the beam direction for protons of 3 GeV/c, 5 GeV/c, 8 GeV/c, 8.9 GeV/c (Be only), 12 GeV/c and 12.9 GeV/c (Al only) beam momentum impinging on thin (5% interaction length) beryllium, carbon, aluminium, copper, tin, tantalum and lead targets using the full data sets was published in [17]. This publication contains a large amount of interesting information, here we stress only some interesting features. The secondary pion yield was measured in a large angular and momentum range and double-differential cross-sections were obtained.

In addition the integrated π^-/π^+ ratio in the forward direction was evaluated (see Fig. 4) as a function of the secondary momentum. In the covered part of the momentum range in most bins more π^+'s are produced than π^-'s. In the p–Ta and p–Pb data the ratio is closer to unity than for the p–Be, p–C and p–Al data. The π^-/π^+ ratio is larger for higher incoming beam momenta than for lower momenta.

In particular in the tantalum and lead data, the number of π^+'s produced is smaller than the number of π^-'s in the lowest momentum bin (100 MeV/c–150 MeV/c) for the 8 GeV/c and 12 GeV/c incoming beam momenta. A similar effect was seen by E910 in their p–Au data [26]. Lighter targets do not show this behavior.

The data taken with the lead and tantalum targets are relevant for the optimization of the targetry of a Neutrino Factory, so these results have a direct impact on the design of the machine. The pion yield increases with momentum and in our kinematic range the optimum is between 5 GeV/c and 8 GeV/c.

The use of a single detector for a range of beam momenta makes it also possible to measure the dependence of the pion yield on the secondary particle momentum and emission angle θ with high precision (see [17] for more details).

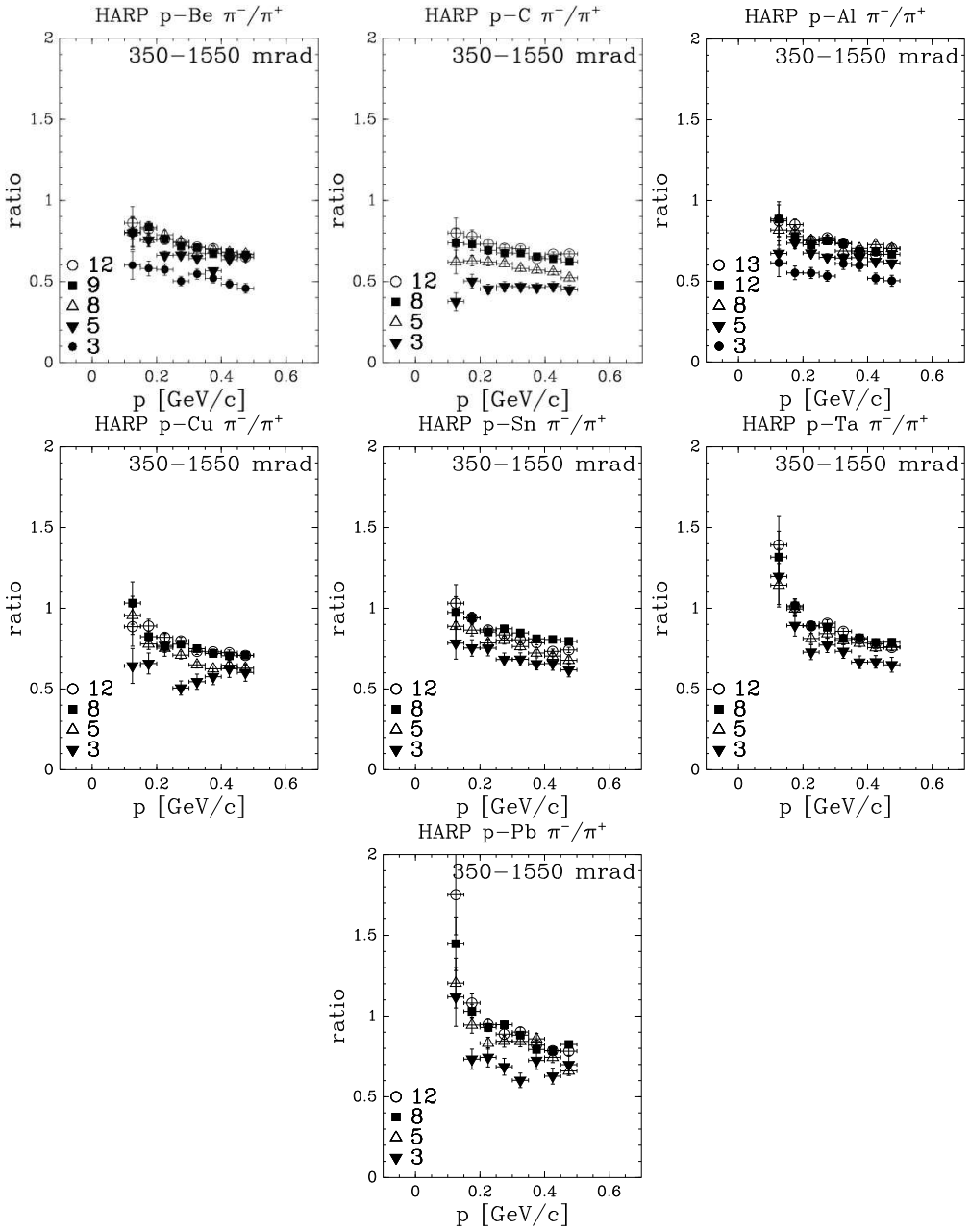

Figure 4: From top-left panel to bottom-right panel, the ratio of the differential cross-sections for π^- and π^+ production in p–Be, p–C, p–Al, p–Cu, p–Sn, p–Ta and p–Pb interactions as a function of the secondary momentum integrated over the forward angular region (shown in mrad). In the figure, the symbol legends empty circles and filled squares refer to 12.9 and 8.9 GeV/c nominal beam momentum, respectively.

3.2 Comparisons with MC predictions

In the following we will show only some comparisons between our results a publicly available Monte Carlo simulations: GEANT4 [23] and MARS [24], using different models.

We stress that no tuning to our data has been done by the GEANT4 or MARS teams. The comparison was done for a limited set of C and Ta targets, as examples of a light and a heavy target nucleus. One of this comparison is shown in Fig. 5.

At intermediate energies (up to 5-10 GeV), GEANT4 uses two types of intra-nuclear cascade models: the Bertini model [27, 28] (valid up to $\sim$ 10 GeV) and the binary model [29] (valid up to $\sim$ 3 GeV). Both models treat the target nucleus in detail, taking into account density variations and tracking in the nuclear field. The binary model is based on hadron collisions with nucleons, giving resonances that decay according to their quantum numbers. The Bertini model is based on the cascade code reported in [30] and hadron collisions are assumed to proceed according to free-space partial cross sections and final state distributions measured for the incident particle types.

At higher energies, instead, two parton string models, the quark-gluon string (QGS) model [27, 31] and the Fritiof (FTP) model [31] are used, in addition to a High Energy Parametrized model (HEP) derived from the high energy part of the Gheisha code used inside GEANT3 [32].

A realistic GEANT4 simulation is built by combining models and physics processes into what is called a "physics list". In high energy calorimetry the two most commonly used are the QGSP physics list, based on the QGS model, the pre-compound nucleus model and some of the Low Energy Parametrized (LEP) model (that has its root in the GHEISHA code inside GEANT3) and the LHEP physics list [33] based on the parametrized LEP model and HEP models.

The MARS code system [24] uses as basic model an inclusive approach multi-particle production originated by R. Feynman. Above 3 GeV/c phenomenological particle production models are used. Below 5 GeV/c a cascade-exciton model [34] combined with the Fermi break-up model, the coalescence model, an evaporation model and a multi-fragmentation extension is used instead.

None of the considered models describe fully our data. However, backward or central region production seems to be described better than relatively more forward production, especially at higher incident momenta. In our data, the lowest angular bin corresponds to a transition region from forward to central production, that is more difficult to describe by MC models.

In general, π^+ production is better described than π^- production. At higher energies the FTP model (from GEANT4) and the MARS model describe better the data, while at the lowest energies the Bertini and binary cascade models (from GEANT4) seem more appropriate. Parametrized models, as LHEP from GEANT4, show relevant discrepancies: up to a factor of three in the forward region at low energies.

The comparison, just outlined in our paper, between data and models shows that the full set of HARP data, taken with targets spanning the full periodic table of elements, with small total errors and large coverage of the solid angle with a single detector, may greatly help the tuning of models used in hadronic simulations in the difficult energy range between 3 GeV/c and 15 GeV/c of incident momentum.

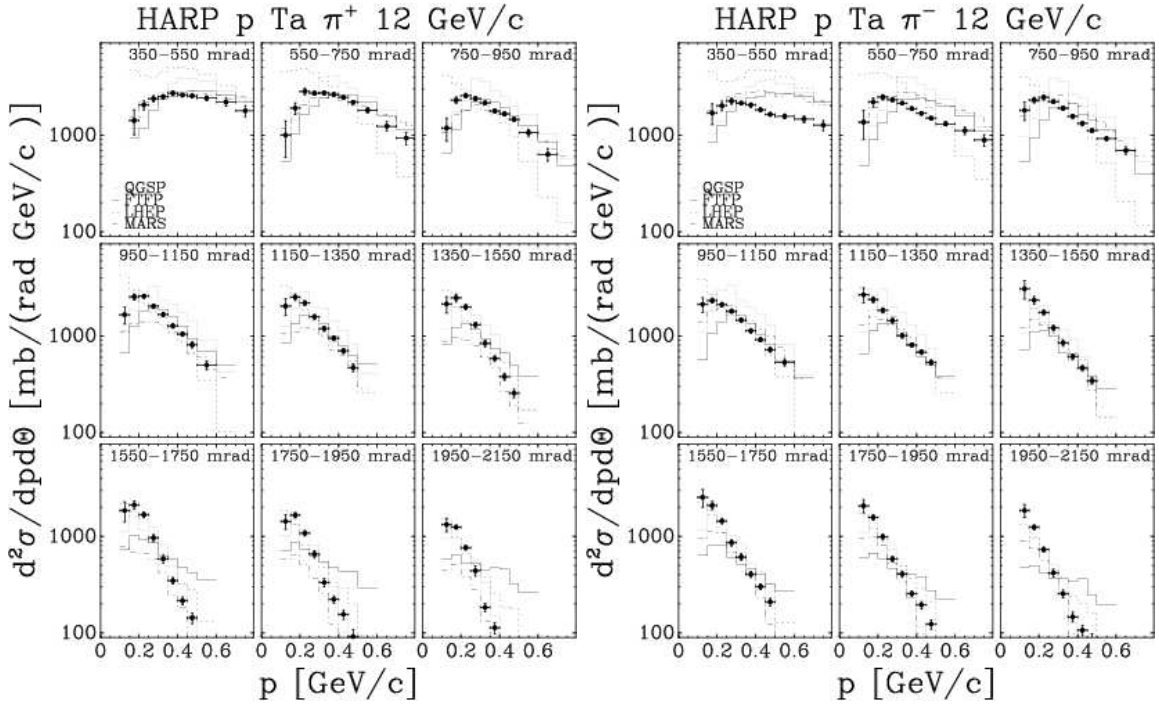

Figure 5: Comparison of HARP double-differential $\pi^{\pm}$ cross sections for p–Ta at 12 GeV/c with GEANT4 and MARS MC predictions, using several generator models (see text for details).

4 Large Angle region: Cross sections comparison with existing data

4.1 Comparisons with earlier data

Very few pion production data sets are available in the literature for proton interactions in this energy region and in general suffer from large systematic and statistical uncertainties, except for E910 [26] and Shibata *et al.* [35]. A comparison of these results with the published HARP data is reported here.

4.1.1 p–C Data

Our data can be compared with results from Ref. [36] and [37] where measurements of π^- production are reported in 4.2 GeV/c and 10 GeV/c p–C interactions, respectively. The total number of π^- observed in the above references is about 1300 (5650) in the 4.2(10) GeV/c data[1]. In the papers cited above no tables of the double differential cross-sections were provided, the measurements being given in parametrized and graphical form only. The authors of Ref. [36] and [37] give the results as a simple exponential in the invariant cross-section: $\frac{E}{A}\frac{\mathrm{d}^3\sigma}{\mathrm{d}p^3}$, where E and p are the energy and momentum of the produced particle, respectively, and A the atomic number of the target nucleus[2]. Unfortunately, no absolute normalization is given numerically.

[1] more than one order of magnitude smaller of the corresponding HARP data sets

[2] their spectra are parametrized in each angular bin with a function of the form $f_{\pi^-} = c\ \exp(-T/T_0)$, where T is the kinetic energy of the produced particle and T_0 is given by $T_0 = T'/(1-\beta\ \cos\theta)$. For the 4.2 GeV/$c$ data

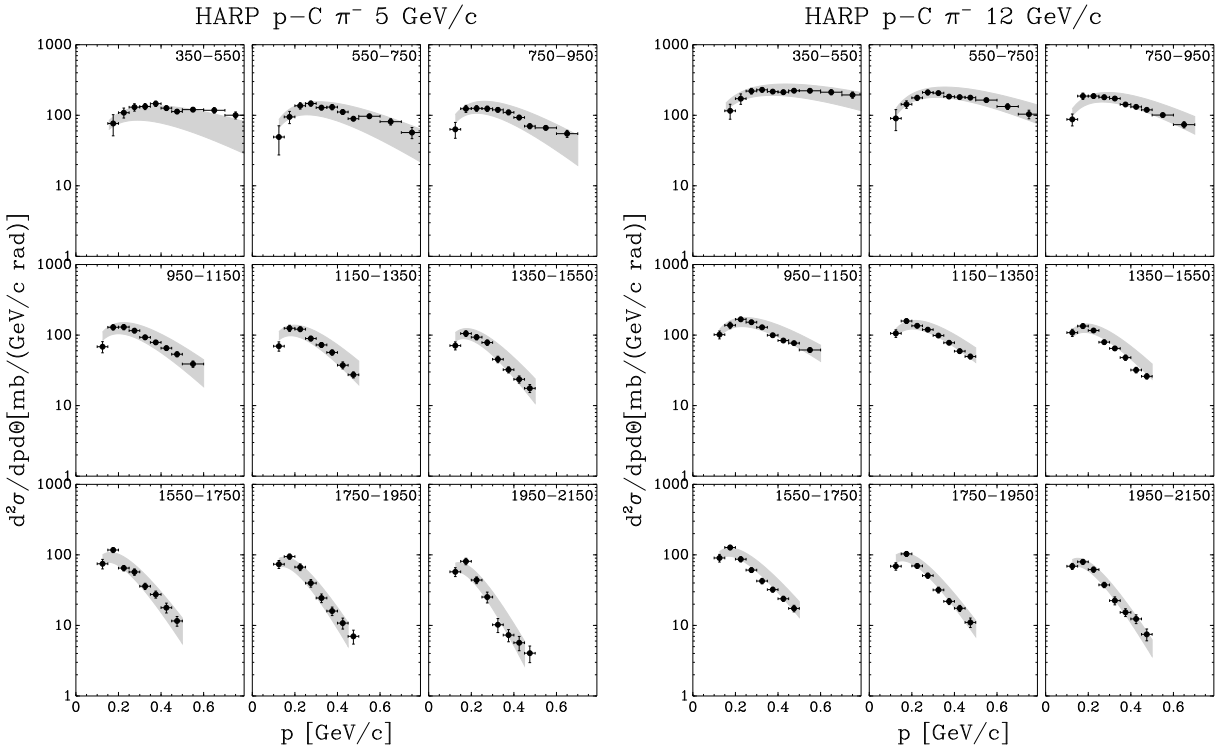

Figure 6: Comparison of the HARP p–C results with data from Ref. [36] and [37]. The left panel shows the comparison of the parametrization of the 4.2 GeV/c data of Ref. [36] with the 5 GeV/c HARP data; the right panel shows the comparison of the 10 GeV/c parametrization of [37] with the 12 GeV/c data. The absolute normalization of the parametrization was fixed to the data in both cases. The band shows the range allowed by varying the slope parameters given by [36] and [37] with two standard deviation and a 10% variation on the absolute scale. The angular ranges are shown in mrad in the panels.

To provide a comparison with these data, the parametrization was integrated over the angular bins used in our analysis and with an arbitrary overall normalization overlaid to our results. We compare the 4.2 GeV/c parametrization of Ref. [36] with our 5 GeV/c data and the Ref. [37] parametrization with our 12 GeV/c data. Only the comparison of the slopes with secondary momentum can be considered significant.

Our p–C data can also be compared with π^+ and π^- production measurements taken with 12 GeV/c incident protons from Ref. [35]. These data were taken with a magnetic spectrometer and only measurements at 90 degrees from the initial proton direction are available. The statistical point–to–point errors are quoted to be 3%, while the overall normalization has a 30% uncertainty due to the knowledge of the acceptance. In Fig. 7 their p–C data are shown together with the HARP p–C data. The filled boxes show the data directly from Ref. [35], while the open boxes are scaled with a factor 0.72. This factor was defined by scaling the average of the π^- and π^+ data from Ref. [35] at 179 MeV/c and 242 MeV/c to the HARP data averaged over the same region. The scale factor is within one standard deviation of the systematic normalization uncertainty of Ref. [35]. The latter data set compares well with the data described in this paper (filled circles) in the angular region 1.35 rad $\leq \theta <$1.55 rad at the same proton beam momentum.

the values of the parameters are $T' = (0.089 \pm 0.006)$ GeV/c and $\beta = 0.77 \pm 0.04$ and $T' = (0.100 \pm 0.002)$ GeV/c and $\beta = 0.81 \pm 0.02$ for the 10 GeV/c data.

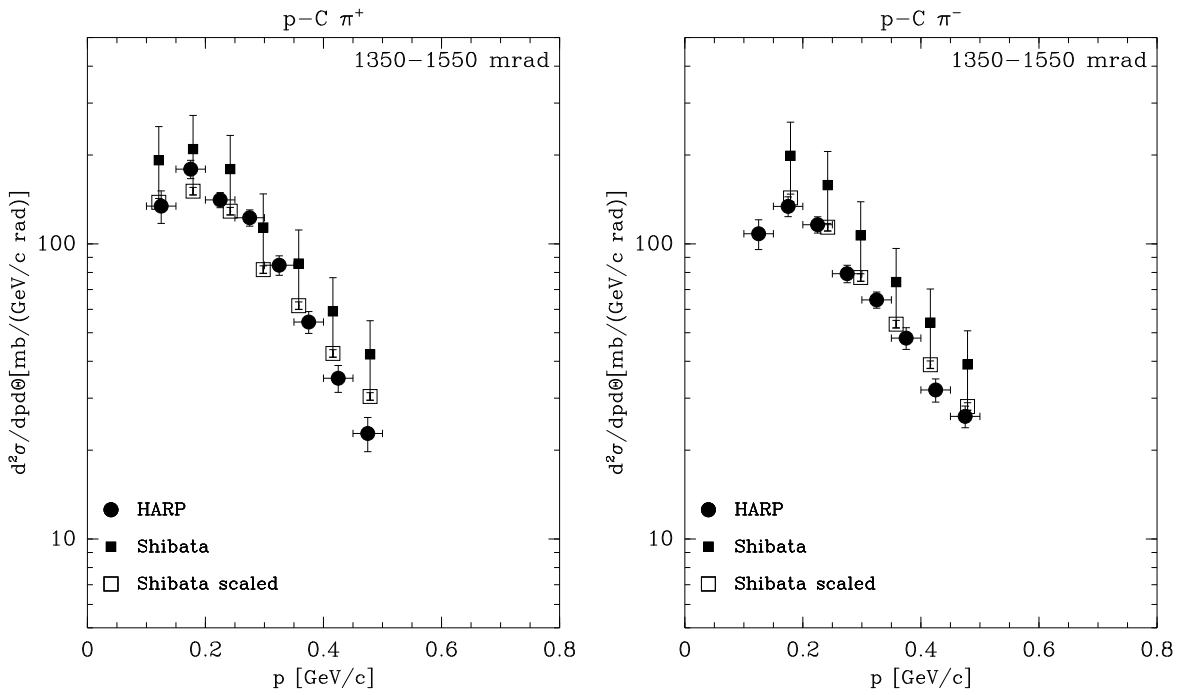

Figure 7: Comparison of the HARP results with π^+ and π^- production data at 90 degrees from Ref. [35] taken with 12 GeV/c protons. The left panel shows the comparison of the π^+ production data of Ref. [35] with the HARP data; the right panel shows the comparison with the π^- production data. The smaller filled boxes show the data directly from Ref. [35], while the open boxes are scaled as explained in the text. The latter data set compares well with the data described in this paper (filled circles) in the angular region 1.35 rad $\leq \theta <$1.55 rad.

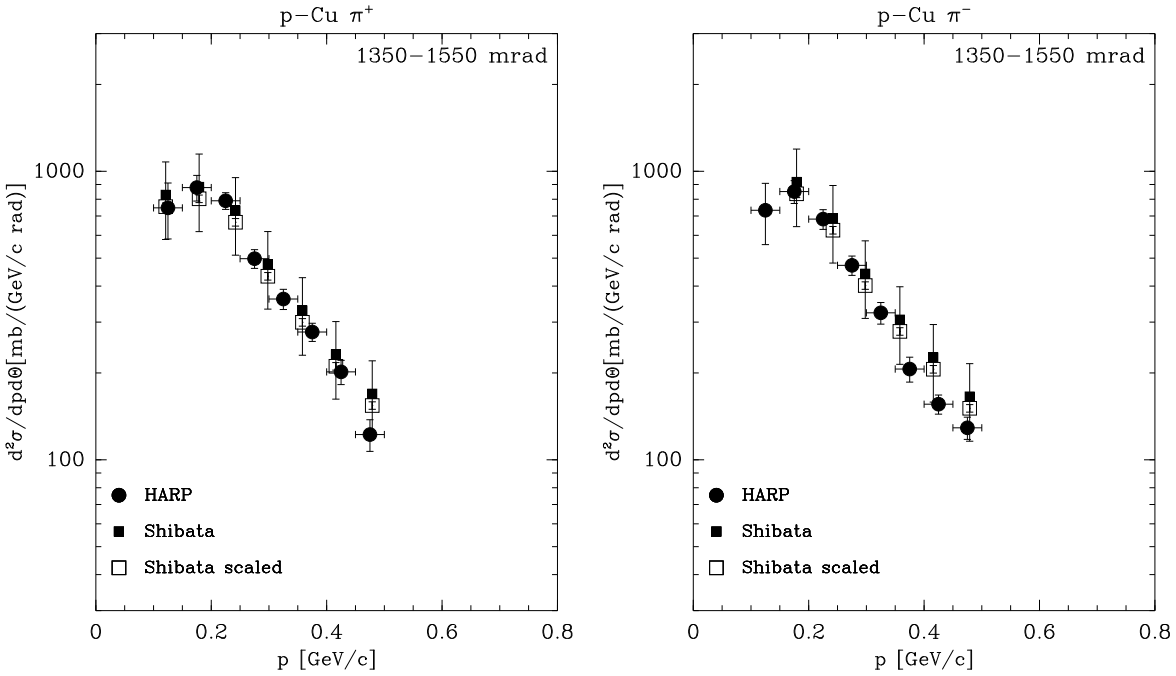

Figure 8: Comparison of the HARP data with π^+ and π^- production data at 90 degrees from Ref. [35] taken with 12 GeV/c protons. The left panel shows the comparison of the π^+ production data of Ref. [35] with the HARP data; the right panel shows the comparison with the π^- production data. The smaller filled boxes show the data directly from Ref. [35], while the open boxes are scaled as explained in the text. The latter data set compares well with the data described in this paper (filled circles) in the angular region 1.35 rad $\leq \theta <$1.55 rad.

4.1.2 p–Cu Data

Our p–Cu data can be compared with π^+ and π^- production measurements taken with 12 GeV/c incident protons from Ref. [35]. In Fig. 8 the p–Cu data of Ref. [35] are shown together with the HARP p–Cu results. The filled boxes show the data directly from Ref. [35], while the open boxes are scaled with a factor 0.91. This factor was defined in a similar procedure as described for the p–C data. The scale factor is very close to unity and well within one standard deviation of the systematic normalization uncertainty of Ref. [35]. Like for the p–C data, the full error bars including the 30% scale uncertainty of Ref. [35] are drawn, for the scaled data only their quoted statistical error of 3% is shown. The agreement of the two data sets is excellent. The fact that the two scale factors are different may be due to the fact that the scale uncertainty in Ref. [35] holds separately for data sets taken with different target nuclei.

Also available data at 12.3 GeV/c from the E910 experiment [26] are in reasonable agreement with our p–Cu results as shown in Fig. 9. In order to take into account the different angular binning which prevent a direct comparison, a Sanford-Wang parametrization is fitted to our data. The fit is performed to the data redefined as $d^2\sigma^\pi/dpd\Omega$. An area between two parametrizations is defined which contains our data points as shown in Fig. 9 (top panels). It is visible that the parametrization is not a perfect description to our data. Therefore, we define a band of $\pm$15% around the best fit which contains almost all the HARP data points. The same parametrizations are then displayed in the binning of E910. While the shape of the distributions are similar for both π^+ and π^- in HARP and E910 data sets, the absolute normalizations disagree by 5%–10%. For the individual data sets the systematic errors are between 5% and 10% depending on the

range of secondary momentum. Since these errors are correlated between bins, the discrepancy in the π^+ and π^- data separately are of the order of one standard deviation.

4.1.3 p–Be Data

The p–Be data at 12.3 GeV/c from the E910 experiment [26] are in reasonable agreement with our results as shown in Fig. 10. Also in this case, to take into account the different angular binning which prevent a direct comparison, a Sanford-Wang parametrization [25] is fitted to our data and the same procedure described for the p–Cu data is applied (see Fig. 10 (top panels)). The same parametrizations are then displayed in the binning of E910. While the shape of the distributions are similar for both π^+ and π^- in the HARP and E910 data sets, the absolute cross-sections disagree by up to 15% for the π^+ data and agree well for the π^- data. (The parametrization shows similar difficulties to fit both π^- data sets). One should note that the range of the systematic errors of the HARP data is 5% to 10% and similar for the E910 data, such that the disagreement is not much larger than one standard deviation [3].

4.1.4 p–Al Data

Our p–Al data have been compared with π^+ and π^- production measurements at 12 GeV/c incident proton momentum from Shibata *et al.* [35]. Their data were taken with a magnetic spectrometer and only measurements at 90 degrees from the initial proton direction are available. The statistical point–to–point errors are quoted to be 3%, while the overall normalization has a 30% uncertainty due to the knowledge of the acceptance. In Fig. 11 their data are shown together with the HARP results. Their data set compares well with the HARP data (filled circles) in the angular region 1.35 rad $\leq \theta <$1.55 rad at the same proton beam momentum[4].

4.2 Comparisons with the HARP Forward region results

Unfortunately the HARP forward (FW) and Large Angle (LA) spectrometers do not have any angular overlap. However they have a common momentum region between 0.5 GeV/c and 0.75 GeV/c that allow us to present on the same plot the double differential cross-sections provided by the FW and LA spectrometers in different angular bins.
As an example, in Fig. 12 (left panel) the results for secondary π^+ productions of p–Be at 8.9 GeV/c are shown for both FW (filled squares) and LA (filled circles) angular bins. Compared to the published LA data, one more forward angular bin (open circle) was added to improve the shape knowledge. A good agreement in the results obtained with the two HARP spectrometers is clearly visible.
It is also possible to study many other dependencies like, for example, the π^+/π^- ratio as a function of the polar angle. In Fig. 12 (Right panel) the π^+/π^- ratio is shown for p–Be data taken with 12 GeV/c incident protons. In this last case, it was possible to compare our results with those provided by the E910 experiment [26], that are available for almost the same (12.3 GeV/c) proton momentum.
The agreement is good. Only one bin exhibit a visible discrepancy but given the large error it

[3] As a side remark, E910 data shows a step around 800 MeV/c in momentum (inverse for π^+, π^-) that may explain also the observed discrepancy.

[4] In this comparison data are compared with their proper experimental normalization factors, while in the previous published comparison of our carbon and copper target data with their data sets normalization factors 0.72 (0.91) were used, still compatible with their overall quoted normalization uncertainty of 30%.

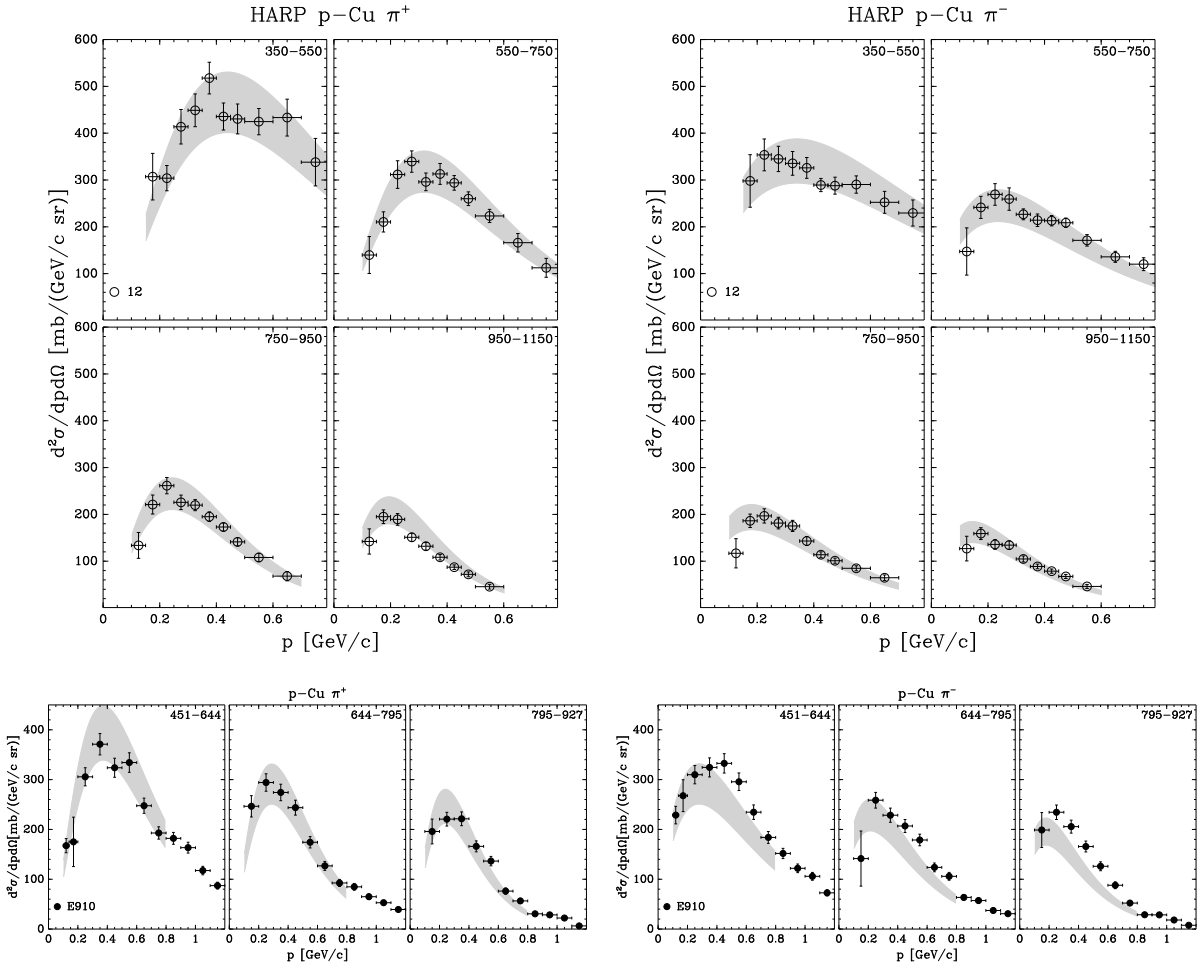

Figure 9: Comparison of the HARP data with π^+ and π^- production data from Ref. [26] taken with 12.3 GeV/c protons. The top panels show a parametrization of the π^+ (left) and π^- (right) production data described in this paper. The data have been normalized to represent $\mathrm{d}^2\sigma^\pi/\mathrm{d}p\mathrm{d}\Omega$. The shaded band represents the area between two parametrization which contain the data points. The bottom panels show the comparison of the same parametrization, now binned according to the E910 data. The bottom left (right) panel shows the π^+ (π^-) production data of Ref. [26]. The angular regions are indicated in mrad in the upper right-hand corner of each plot.

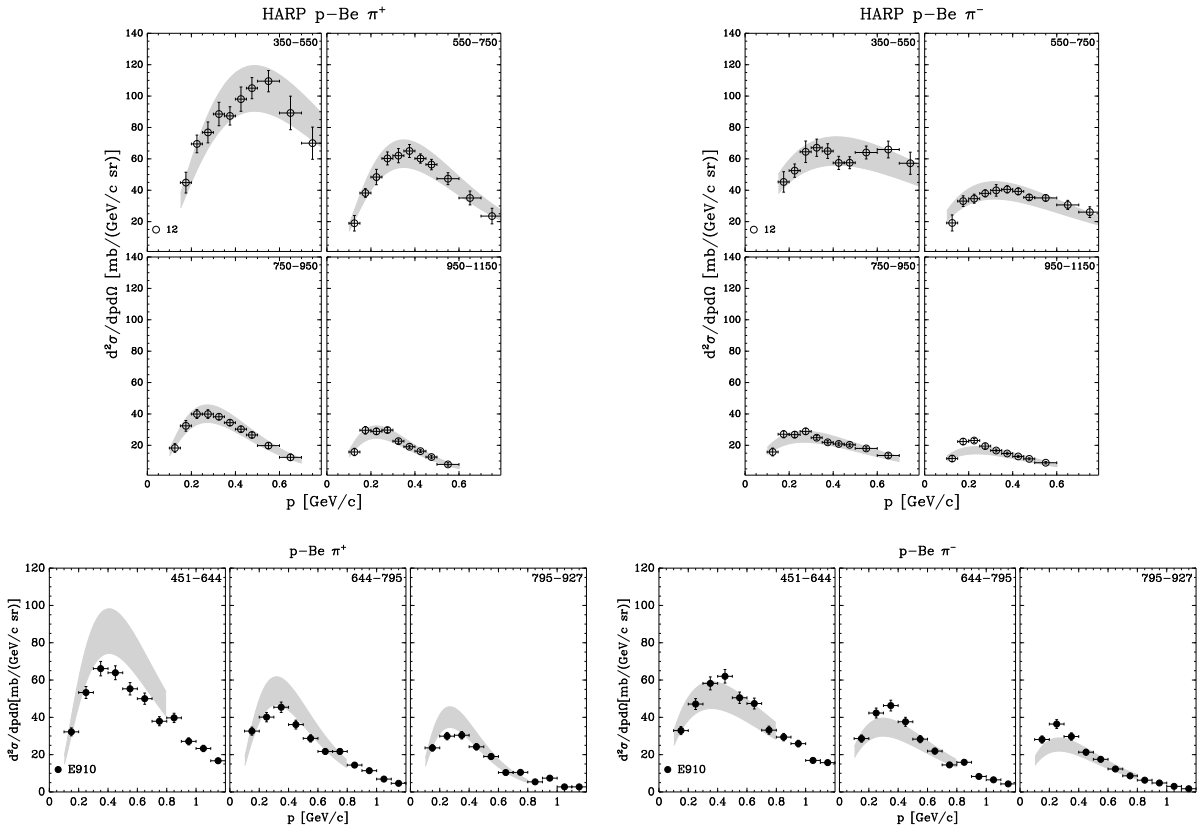

Figure 10: Comparison of the HARP Be data with π^+ and π^- production data from Ref. [26] taken with 12.3 GeV/c protons. The top panels show a parametrization of the π^+ (left) and π^- (right) production data described in this paper. The data have been normalized to represent $\mathrm{d}^2\sigma^\pi/\mathrm{d}p\mathrm{d}\Omega$. The shaded band represents the area between two parametrization which contain the data points. The bottom panels show the comparison of the same parametrization, now binned according to the E910 data. The bottom left (right) panel shows the π^+ (π^-) production data of Ref. [26]. The angular regions are indicated in mrad in the upper right-hand corner of each plot.

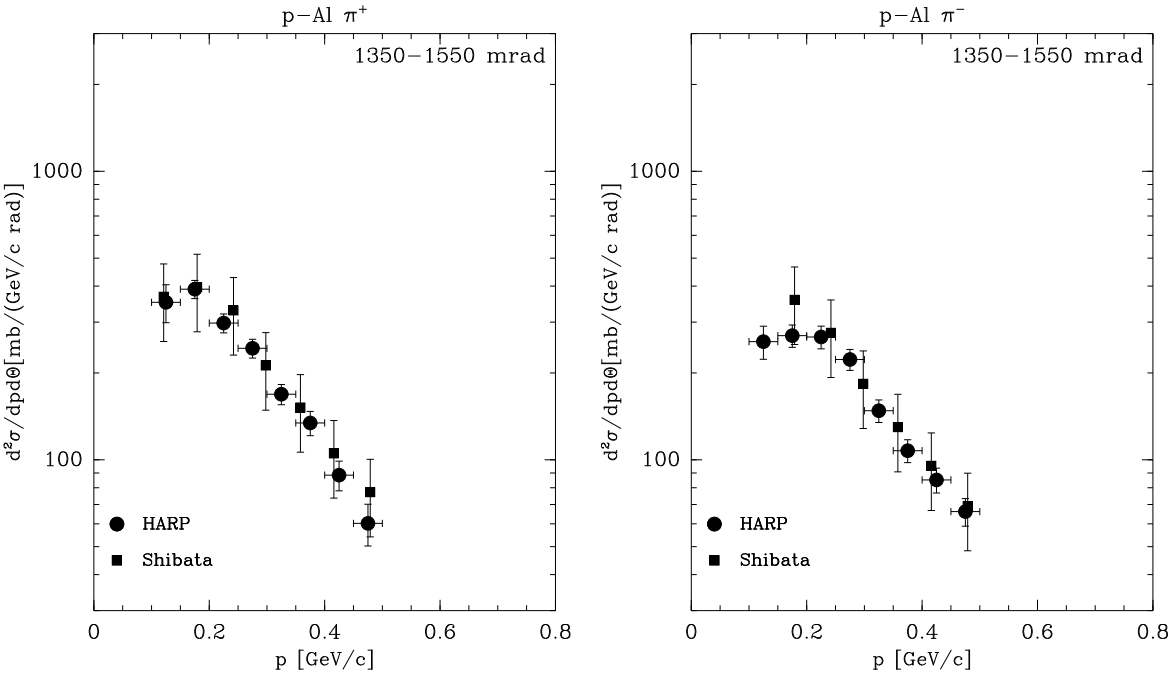

Figure 11: Comparison of HARP p–Al data with π^+ and π^- production data at 90 degrees from Ref. [35] taken with 12 GeV/c incident protons. The left panel shows the comparison of the π^+ production data of Ref. [35] with the HARP data; the right panel shows instead the comparison with the π^- production data. The data sets compares well with our results (filled circles) in the angular region $1.35 \leq \theta < 1.55$ rad.

is still compatible.

4.3 Comparisons with results obtained by the splinter group

In the 2003 Dr. F.Dydak (CERN), the day after he lost an election as spokesperson, started working on his own, setting up a small group of physicists under his control from CERN, Dubna and Protvino, keeping them forcibly isolated from the rest of HARP[5]. While they had full access to HARP data, collaboration software, meeting minutes and transparencies, and internal notes, they systematically refused in spite of repeated invitations, to attend analysis meetings and present or discuss their results. In the following we will refer to this group as the splinter group. We, HARP Collaboration, consider this situation unacceptable and we denounced it several times.

However, following the request of our SPSC referees, we have accepted to produce comparisons between our results (completed more than 2 year ago and later on published) with cross-sections of the production of secondary charged pions on Beryllium target with proton beam at 5 GeV/c, 8.9 GeV/c, 12 GeV/c recently obtained by the splinter group. The data points have been taken from [38, 39, 40] and the same angular dΩ (in degrees) and transverse momentum bins used by the authors are applied. The results are shown in Figs. 14, 15, 16 for proton beam momenta of 5, 8.9 and 12 GeV/c respectively.

It should be stressed that the HARP data are tabulated in dθ bins and momentum. In addition

[5]During all these years this group acted completely independent from the HARP collaboration and received financial support directly from the CERN management

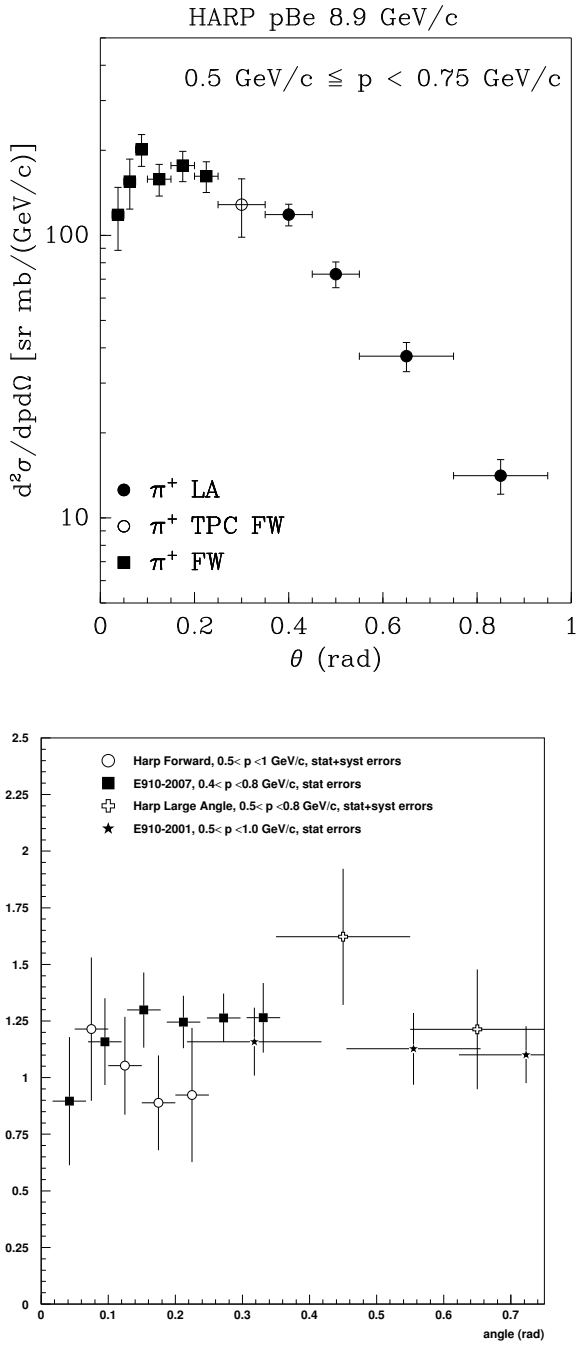

Figure 12: Left panel: double differential cross-sections for secondary π^+ productions of p–Be at 8.9 GeV/c for both HARP FW (filled squares) and LA (filled circles) angular bins. Compared to the published LA data, one more forward angular bin (open circle) was added. Right panel: π^+/π^- ratio as a function of the polar angle for p–Be data taken with 12 GeV/c incident protons:HARP FW angular bins (open circles), LA angular bins (open crosses), E910 (filled squares(FW) and filled stars (LA)).

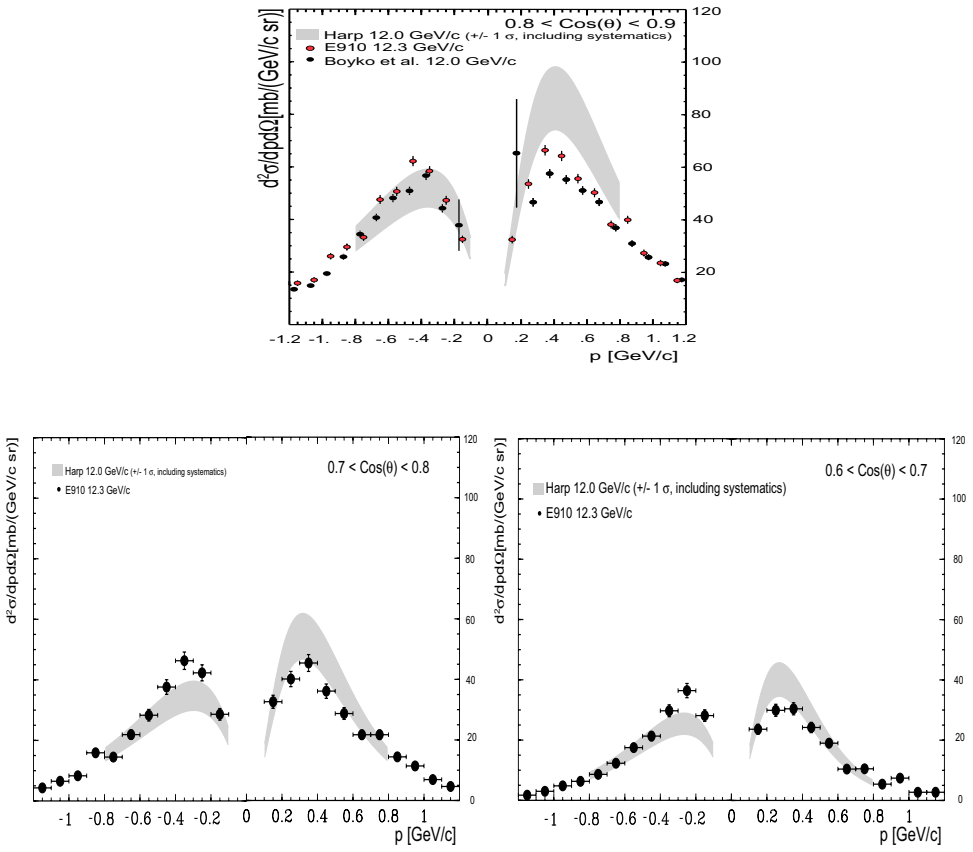

Figure 13: Comparison of the HARP Be data with π^+ and π^- production data from Ref. [26] taken with 12.3 GeV/c protons. The data have been normalized to represent $\mathrm{d}^2\sigma^\pi/\mathrm{d}p\mathrm{d}\Omega$. The shaded band represents the area between two parametrization which contain the data points binned according to the E910 data of Ref. [26]. The angular regions are indicated in the upper right-hand corner of each plot. Only for the froward region bin (top) some CDP recent results are available [38] and have been included in the plot.

the angular bins are expressed in radians and have different amplitudes. For this reason to make the comparisons we were obliged to apply several conversions and some approximations. In particular the changes in the migration matrix and in the background subtraction cannot be taken properly into account. However, we believe that the results are roughly correct.

The π^- data seem to be in reasonable agreement in the full angular range for all the available proton beam momenta. The π^+ data show a different behavior: for 5 GeV/c data they seem to agree for θ larger than 50-55 degrees but not in the very forward region.
Without open and deep discussions and exchanges between the CDP and the HARP, it is difficult for us to understand this. However we notice that the errors quoted in [39, 40] seem far from being realistic. We believe that the apparent difference can be reduced when a more final evaluation of the systematics (that are quite large in this angular region) will be done by the splinter group.
The misidentification of protons as pions advocated by F.Dydak et al. seems not be supported by the data.
In this last case the effect should be visible in the whole angular range and should be larger at higher momenta (when it is much more difficult to discriminate between protons from pions using the dE/dx) than vice-versa.
In conclusion the differences between the two results seems to be confined to π^+ data in the forward region where the systematic errors are larger. If we compare the results obtained by both analyses in the forward region with the corresponding measurement published in [26] we discover that the E910 data are more or less in the middle and and do not really help to solve the puzzle (see Fig. 13 top panel). However as shown in Fig. 10 the range of the systematic errors of the HARP data is 5% to 10% and similar for the E910 data, such that the disagreement between them is not much larger than one standard deviation.

5 HARP Publications

5.1 Detector description and Reconstruction methods

1. The HARP detector at the CERN PS.

   M.G.Catanesi et al :Nucl.Instrum.Meth.A571:527-561,2007.

2. Particle identification algorithms for the HARP forward spectrometer.

   M.G.Catanesi et al : Nucl.Instrum.Meth.A572:899-921,2007.

3. The time-of-flight TOFW detector of the HARP experiment: Construction and performance.

   M.Baldo-Ceolin et al.: Nucl.Instrum.Meth.A532:548-561,2004.

4. Physics performance of the barrel RPC system of the HARP experiment.

   M. Bogomilov et al. : IEEE Trans.Nucl.Sci.54:342-353,2007.

5. The Time Response of Glass Resistive Plate Chambers to Heavily Ionizing Particles.

   A. Artamonov et al.:JINST 2:P10004,2007.

6. Absolute momentum calibration of the HARP TPC.

   M.G.Catanesi et al.:(arXiv:0709.2806) 2008 JINST 3 P04007

5.2 Physics Results

1. Measurement of the production cross-section of positive pions in p-Al collisions at 12.9-GeV/c

   M.G.Catanesi et al.:Nucl.Phys.B732:1-45,2006. (K2K)

2. Measurement of the production of charged pions by protons on a tantalum target.

   M.G Catanesi et al.:Eur.Phys.J.C51:787-824,2007.

3. Measurement of the production cross-section of positive pions in the collision of 8.9 GeV/c protons on beryllium.

   M.G Catanesi et al.:Eur.Phys.J.C52:29-53,2007. September 2007 (MiniBoone)

4. Large-angle production of charged pions by 3 GeV/c 12 GeV/c protons on carbon, copper and tin targets

   M.G.Catanesi et al.:Eur.Phys.J.C53:177-204,2008. January 2008

5. Large-angle production of charged pions by 3-12.9 GeV/c protons on beryllium, aluminium and lead targets.

   M.G.Catanesi et al.: Eur.Phys.J.C54:37-60,2008.

6. Measurement of the production cross-sections of $\pi^{\pm}$ in p-C and $\pi^{\pm}$-C interactions at 12 GeV/c.

   M.G.Catanesi et al.:Astroparticle Physics - volume/issue: 29/4 pp. 257-281

7. Forward production of $\pi^{\pm}$ in p-O2 and p-N2 interactions at 12 GeV/c.

   M.G. Catanesi et al.:Astropart.Phys.30:124-150,2008.

8. Large-angle production of charged pions with 3-12.9 GeV/c incident protons on nuclear targets.

   M.G.Catanesi et al.:Phys.Rev.C 77:055207,2008

9. Forward production of charged pions with incident π^{+} and π^{-} on nuclear targets measured at the CERN PS.

   M.G.Catanesi et al.:Accepted for publication in Nucl.Phys.A.

6 Appendix

References

[1] M.G. Catanesi *et al.* [HARP Collaboration], Status report of the HARP experiment, CERN-SPSC-2007-025; 29 September 2007.

[2] E. Aliu *et al.* [K2K Collaboration], Phys. Rev. Lett. **94** (2005) 081802 [arXiv:hep-ex/0411038].

[3] A. A. Aguilar-Arevalo [MiniBooNE Collaboration], Phys. Rev. Lett. 98, 231801 (2007), arXiv:0704.1500v3.

[4] M. G. Catanesi *et al.* [HARP Collaboration], Nucl. Phys. **B732** (2006) 1 [arXiv:hep-ex/0510039].

[5] M. G. Catanesi *et al.* [HARP Collaboration], Eur. Phys. J. **C52** (2007) 29, arXiv:hep-ex/0702024.

[6] A. A. Aguilar-Arevalo *et al.* [SciBooNE Collaboration], "Bringing the SciBar detector to the Booster neutrino beam," FERMILAB-PROPOSAL-0954, (2006), arXiv:hep-ex/0601022.

[7] M. G. Catanesi *et al.* [HARP Collaboration], "Measurement of the production cross-sections of $\pi^{\pm}$ in p–C and $\pi^{\pm}$–C interactions at 12 GeV/c", Astropart. Phys. **29** (2008) 257-281.

[8] M.G. Catanesi *et al.* [HARP Collaboration], Astropart. Phys. **30** (2008) 124-150.

[9] M.G. Catanesi *et al.* [HARP Collaboration], accepted for publication in Nucl. Phys. A.

[10] M.G. Catanesi *et al.* [HARP Collaboration], Eur. Phys. J. **C51** (2007) 787, arXiv:0706.1600.

[11] M. G. Catanesi *et al.* [HARP Collaboration], "Momentum scale in the HARP TPC", arXiv:0709.1600 [physics.ins-det], JINST 3 P04007 (2008).

[12] M. Bogomilov *et al.*, IEEE Trans. Nucl. Sci., **54** (2007), pp. 342-353

[13] A. Artamonov *et al.*, "The Time Response of Glass Resistive Plate Chambers to Heavily Ionizing Particles", arXiv:0709.3756 [physics.ins-det], JINST 2 P10004 (2007).

[14] M.G. Catanesi *et al.* [HARP Collaboration], "Large-angle production of charged pions by 3 GeV/c–12 GeV/c protons on carbon, copper and tin targets", Eur. Phys. J. **C53** (2008) 177-204.

[15] M.G. Catanesi *et al.* [HARP Collaboration], "Large-angle production of charged pions by 3 Ge/Vc–12 GeV/c protons on beryllium, aluminium and lead targets", Eur. Phys. J. **C54** (2008) 37-60.

[16] A. Bagulia *et al.*, "On the Harp TPC dynamic distortions ", paper in preparation.

[17] M.G. Catanesi *et al.* [HARP Collaboration], "Large-angle production of charged pions in the HARP experiment with incident protons on nuclear targets", Phys. Rev. **C77** (2008) 055207.

[18] M.G Catanesi *et al.* [HARP Collaboration], "Proposal to study hadron production for the neutrino factory and for the atmospheric neutrino flux", CERN-SPSC/99-35, 15 November 1999.

[19] M.G. Catanesi *et al.* [HARP Collaboration], Nucl. Instrum. Meth. **A571** (2007) 527; **A571** (2007) 564.

[20] M. G. Catanesi *et al.* [HARP Collaboration], Nucl. Instrum. Meth. **A572** (2007) 899.

[21] M. H. Ahn *et al.* [K2K Collaboration], Phys. Rev. D **74** (2006) 072003 [arXiv:hep-ex/0606032].

[22] A. A. Aguilar-Arevalo *et al.* [MiniBooNE Collaboration], "The Neutrino Flux prediction at MiniBooNE", arXiv:0806.1449 [hep-ex].

[23] S. Agostinelli *et al.* [GEANT4 Collaboration], Nucl. Instrum. Meth. **A506** (2003) 250.

[24] N.V. Mokhov, S.I. Striganov, "Mars overview", FERMILAB-CONF-07-008-AD, 2007.

[25] J. R. Sanford and C. L. Wang, Brookhaven National Laboratory, AGS internal report, 1967 (unpublished); C. L. Wang, Phys. Rev. Letters 25, 1068 (1970); ibid. 25, 1536(E) (1970).

[26] I. Chemakin *et al.*, E910 Collaboration, Phys. Rev. **C65** (2002) 024904.

[27] D.H. Wright *et al.*, AIP Conf. Proc. 896 (2007) 11.

[28] A. Heikkinen *et al.* e-print physics/0306008.

[29] G. Folger, V. Ivanchenko and H.P. Wellisch, Eur. Phys. J. A21 (2004) 407.

[30] H.W. Bertini, P. Guthrie, Nucl. Phys. **A169** (1971).

[31] G. Folger and H.P. Wellisch, e-print physics/0306007.

[32] H. Fesefeld, Technical report PITHA 85-02, Aachen, 1985.

[33] D.H. Wright *et al.*, AIP Conf. Proc. 867 (2006) 479.

[34] S.G. Mashnik *et al.*, LANL report LA-UR-05-7321, 2005.

[35] T.-A. Shibata *et al.*,Nucl. Phys. **A 408** (1983) 525.

[36] G. H. Agakishiev *et al.*, (in Russian), Sov. J. Nucl. Phys. **51** (1990) 1009; JINR-P1-89-793, 1989.

[37] D. Armutliiski *et al.*, "Hadron spectra in hadron–nucleus collisions" (in Russian), JINR-P1-91-191, 1991.

[38] I.Boyko;arXiv:0810.1395 (October 2008)

[39] A. Bolshakova et al., http://cern.ch/harp-cdp/Bepub.pdf

[40] A. Bolshakova et al., http://cern.ch/harp-cdp/Bepub2.pdf

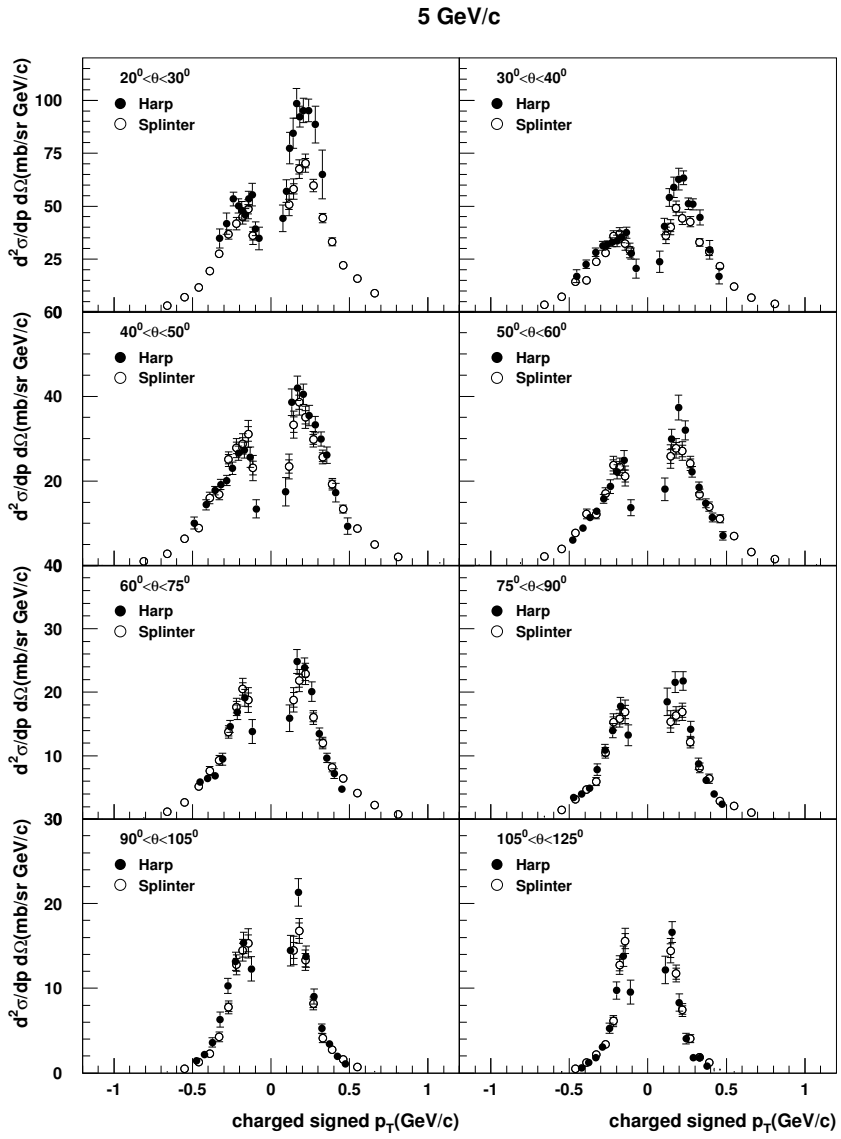

Figure 14: Comparison of the HARP π^+ and π^- production ($\mathrm{d}^2\sigma^\pi/\mathrm{d}p\mathrm{d}\Omega$) in p–Be data at 5 GeV/$c$ (filled circles) with Ref. [40] (empty circles). The angular and transverse momentum bins are the same as used in [40].

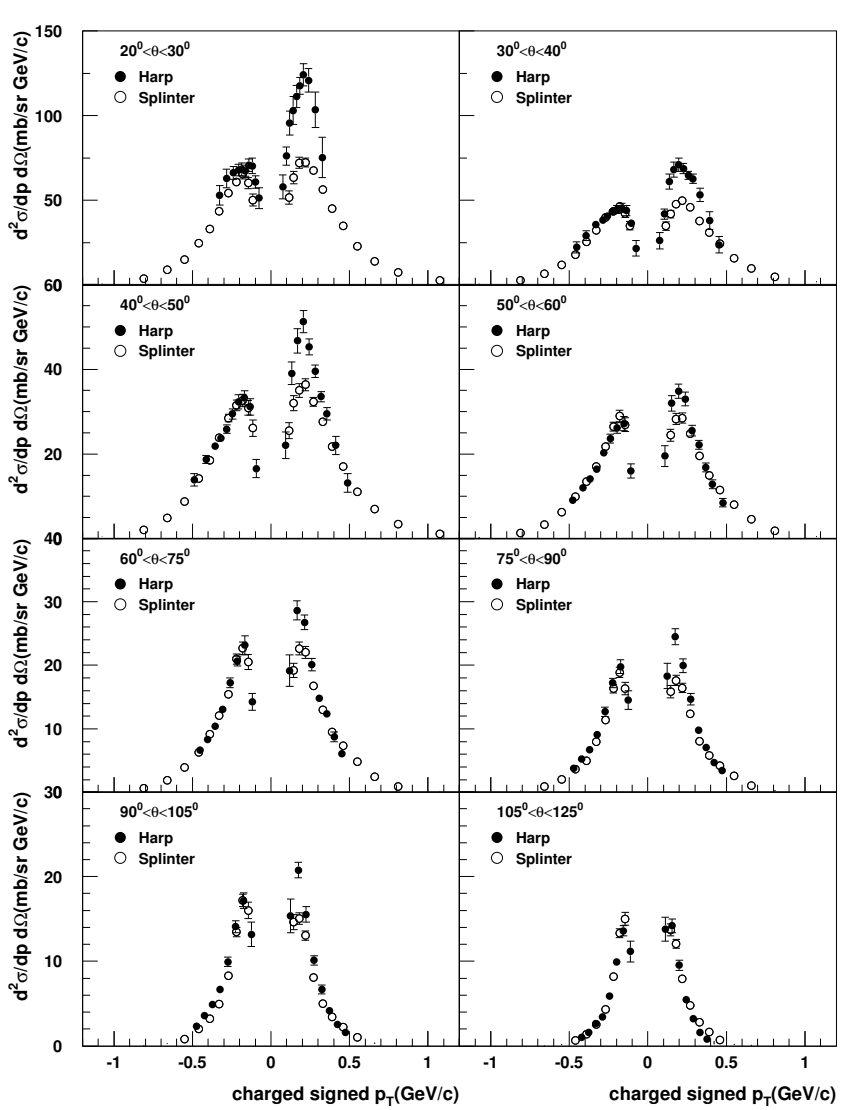

Figure 15: Comparison of the HARP π^+ and π^- production ($\mathrm{d}^2\sigma^\pi/\mathrm{d}p\mathrm{d}\Omega$) in p–Be data at 8.9 GeV/c (filled circles) with Ref. [39] (empty circles). The angular and transverse momentum bins are the same as used in [39].

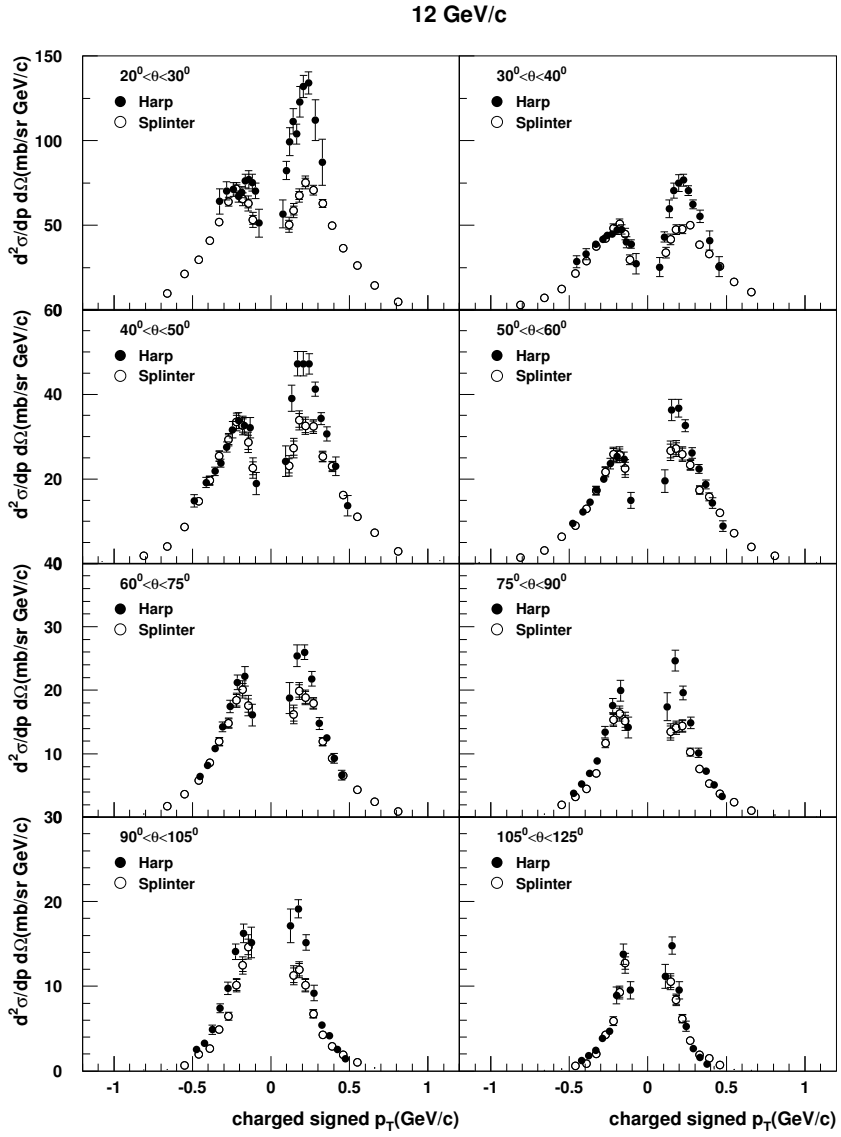

Figure 16: Comparison of the HARP π^+ and π^- production ($\mathrm{d}^2\sigma^\pi/\mathrm{d}p\mathrm{d}\Omega$) in p–Be data at 12 GeV/c (filled circles) with Ref. [40] (empty circles). The angular and transverse momentum bins are the same as used in [40].

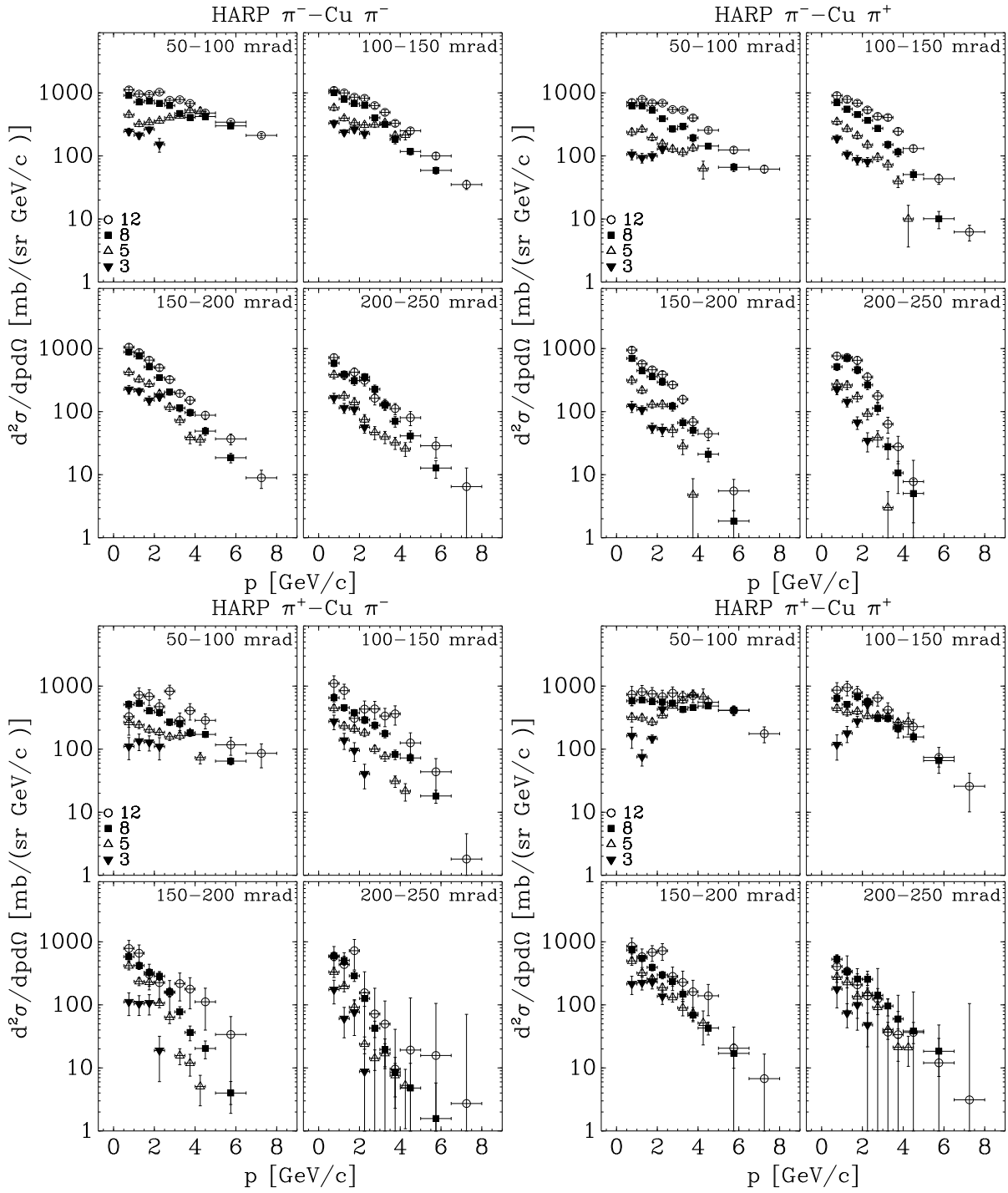

Figure 17: π^-−Cu (top) and π^+−Cu (bottom) differential cross-sections for different incoming beam momenta (from 3 to 12 GeV/c). Left panels show the π^- production, while right panels show the π^+ production. In the top right corner of each plot the covered angular range is shown in mrad.

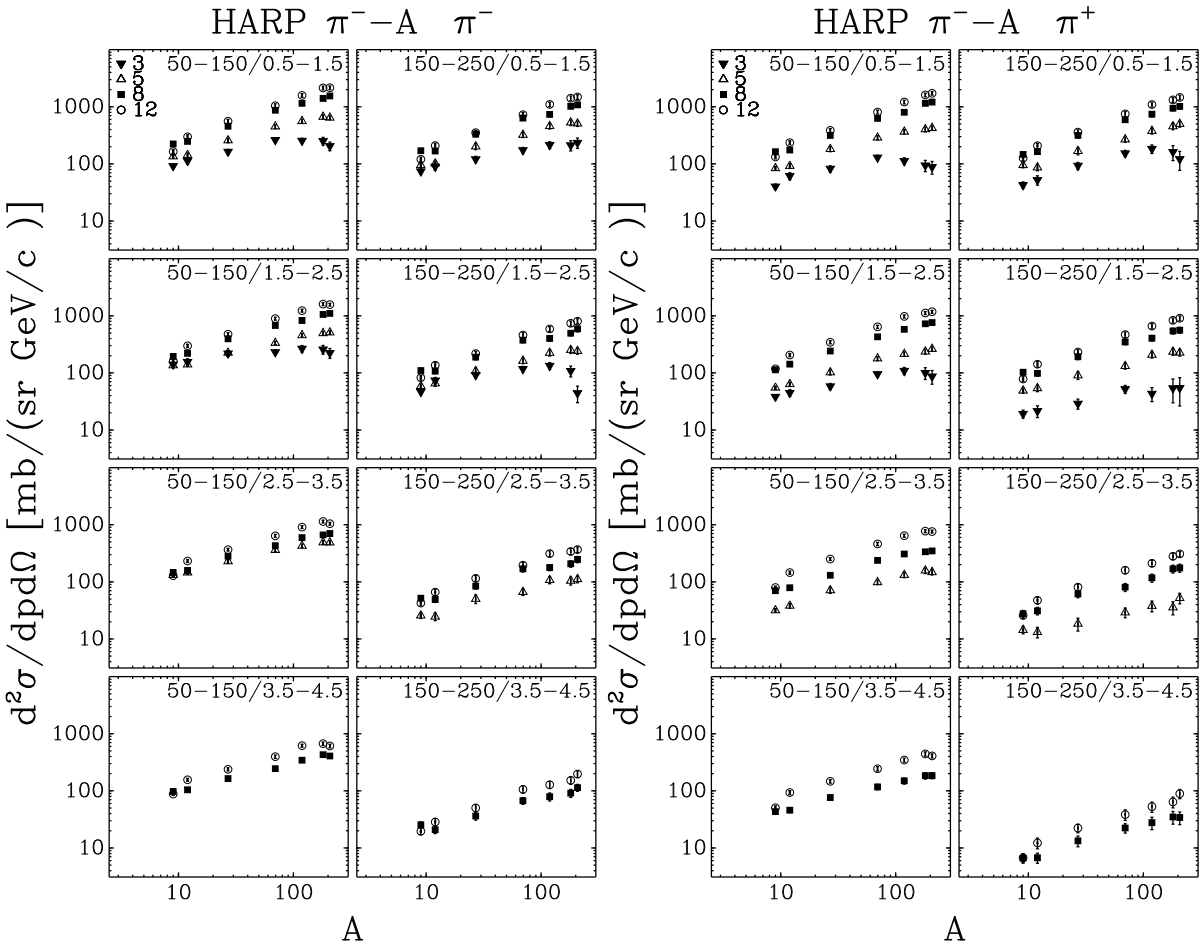

Figure 18: The dependence on the atomic number A of the pion production yields in π^-–Be, π^-–Al, π^-–C, π^-–Cu, π^-–Sn, π^-–Ta, π^-–Pb interactions averaged over two forward angular region (0.05 rad $\leq \theta <$ 0.15 rad and 0.15 rad $\leq \theta <$ 0.25 rad) and four momentum regions (0.5 GeV/$c \leq p <$ 1.5 GeV/c, 1.5 GeV/$c \leq p <$ 2.5 GeV/c, 2.5 GeV/$c \leq p <$ 3.5 GeV/c and 3.5 GeV/$c \leq p <$ 4.5 GeV/c), for the four different incoming beam momenta (from 3 GeV/c to 12 GeV/c).

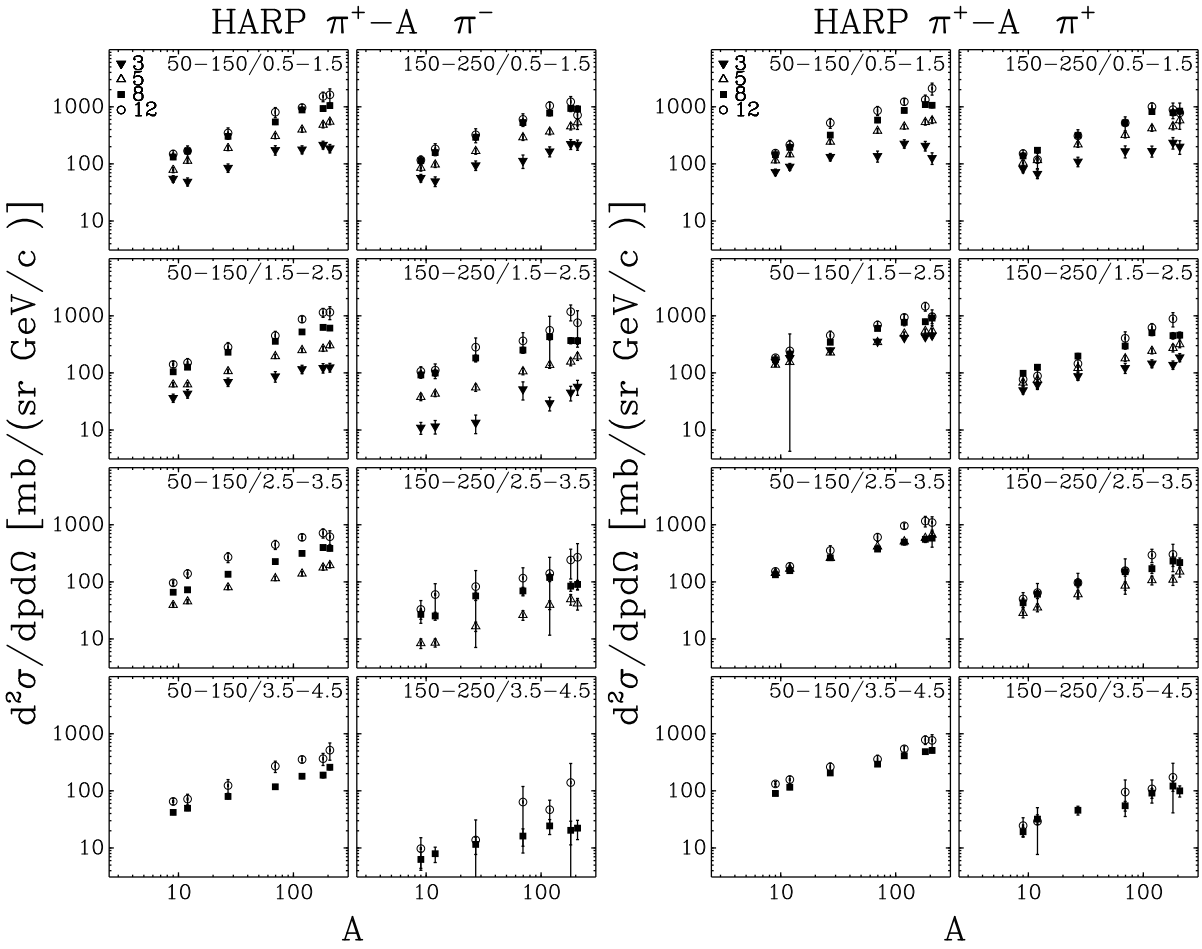

Figure 19: The dependence on the atomic number A of the pion production yields in π^+–Be, π^+–Al, π^+–C, π^+–Cu, π^+–Sn, π^+–Ta, π^+–Pb interactions averaged over two forward angular region (0.05 rad $\leq \theta <$ 0.15 rad and 0.15 rad $\leq \theta <$ 0.25 rad) and four momentum regions (0.5 GeV/$c \leq p <$ 1.5 GeV/c, 1.5 GeV/$c \leq p <$ 2.5 GeV/c, 2.5 GeV/$c \leq p <$ 3.5 GeV/c and 3.5 GeV/$c \leq p <$ 4.5 GeV/c), for the four different incoming beam momenta (from 3 GeV/c to 12 GeV/c).

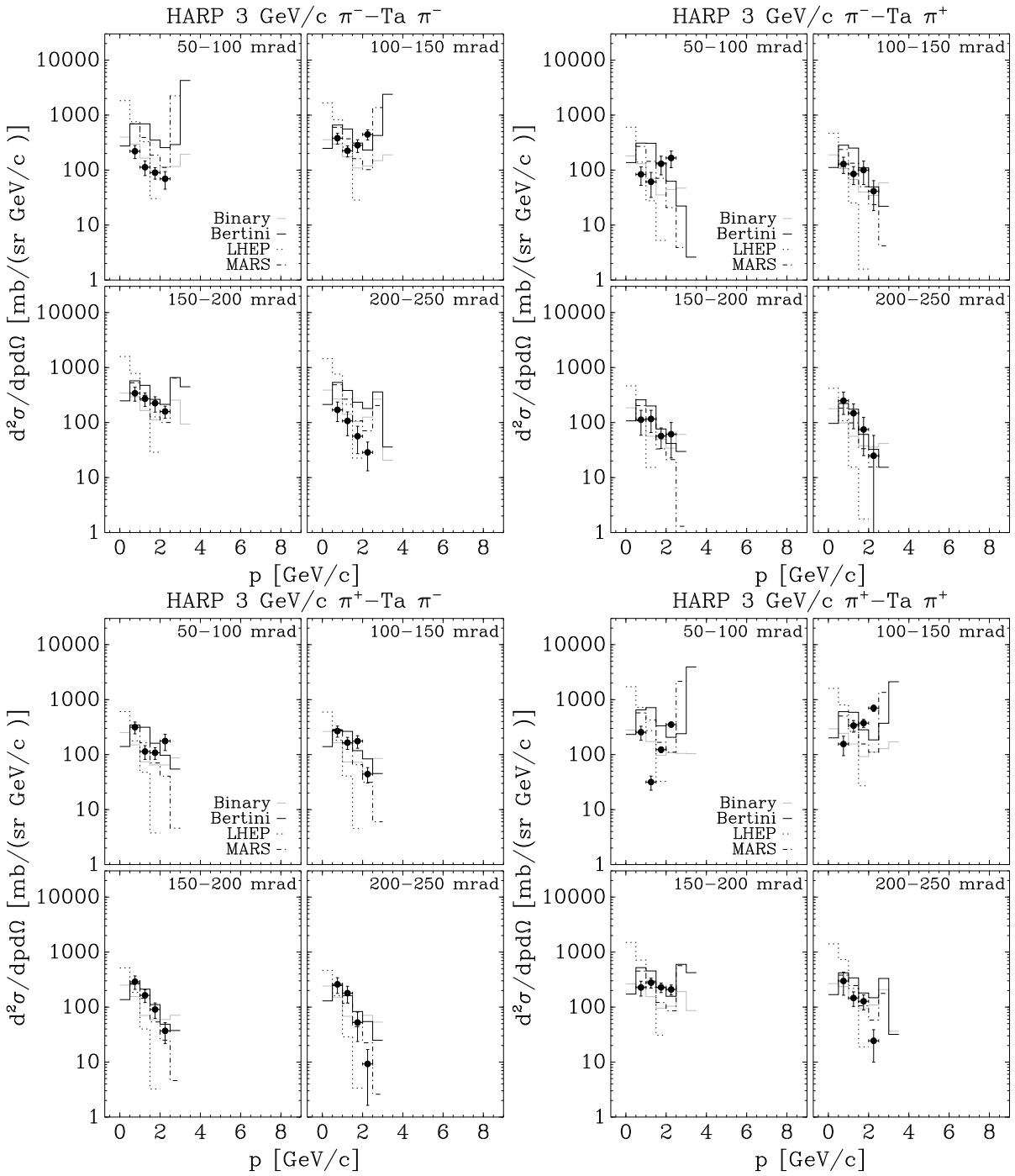

Figure 20: Comparison of HARP double-differential $\pi^{\pm}$ cross-sections for π–Ta at 3 GeV/c with GEANT4 and MARS MC predictions, using several generator models: binary model grey solid line, Bertini model black solid line, LHEP model dotted line, MARS model black dash-dotted line.